IDEA League

Master of Science in Applied Geophysics

Research Thesis

Non-linearity behaviour of soft soil: intermediate-scale laboratory experiments

Stella Cecchi

August 4, 2023

Non-linearity behaviour of soft soil: intermediate-scale laboratory experiments

Master of Science Thesis

for the degree of Master of Science in Applied Geophysics
by

Stella Cecchi

August 4, 2023

IDEA LEAGUE
JOINT MASTER'S IN APPLIED GEOPHYSICS

Delft University of Technology, The Netherlands
ETH Zürich, Switzerland
RWTH Aachen, Germany

Dated: *August 4, 2023*

Supervisor(s):

Dr. van Manen

Prof. Wellmann

Committee Members:

Dr. van Manen

Prof. Wellmann

Abstract

The main aim of this work was to develop methods to estimate quantitatively, and describe qualitatively, the non-linear behaviour of soft soil in intermediate-scale laboratory experiments. Previous works stated that non-linearity of the soil was found for environments involving a large impedance gradient in the near-surface, e.g., a shallow layer of soft, unconsolidated soil overlying a thick harder layer. It is believed that the micro-grains inside the soft soil, in combination with the geometry, caused the non-linearity, although other laboratory experiments found non-linear behaviour for core samples of different single materials.

The novelty of this thesis project lies in the introduction of a new method for investigating the shallow subsurface that has both the advantages of the laboratory environment (e.g., more control over the parameters and higher resolution measurements) and of the field experiments. Therefore, this new, intermediate-scale laboratory approach could be seen as a missing bridge between the experiments on core samples and the field experiments. To the best of our knowledge, this kind of experiment has not been done before and therefore there have not been any physical definitions or classifications of the observed phenomena, yet.

The research was developed in four experiments. The first two experiments verify the scaling, characterize the chosen analogue materials (Clay and Sand), and investigate the influence of the model boundaries. While, the last two experiments focused on the non-linearity behaviour of the soft soil analogues in response to large voltage (e.g., low 100s of Volts) swept-source signals. Overall, we believe we have observed in these experiments several non-linear behaviours for the constructed two layer model; both in terms of a non-linear dependence of the amplitudes on the voltage level as well as in the form of a slowing of the waves for increasing voltage. In addition, we quantify the non-linearity trough a new parameter called the "Non-linearity parameter", γ, and its magnitude describes the level of non-linearity of the soil. The larger γ, the more non-linearly the soil behaves, and vice-versa. A model linearized to first order was used to compare the data measured using an laser Doppler vibrometer with other observed data assuming the linear response. Thanks to that model, we could mathematically generalize the amplitude behaviour of the measured velocities of the soil as a function of γ and visualize the threshold between the linear and non-linear regimes graphically. It appears it is the first time that such parameter is introduced to describe quantitatively the non-linearity.

The proposed methods for investigating the shallow surface by way of intermediate scale analogue models could breathe new life in the use of the physical modeling for near-surface Geophysics. Both the intermediate scale two layer model and the non-linearity parameter appear to be new in this field. The hope is to open a new path for future research keen in understanding better the non linearity behaviour of soft soils.

Acknowledgements

I would like to dedicate this Master Thesis to my siblings, Lorenzo and Gioia, and to my new-born nephews Ariel and Uriele, my angels.

I am very grateful to Dr. Van Manen, who had followed my Thesis project since the begging. He has always believed in me and listened to my idea with a genuine spirit of research. I would never have had the chance to achieve my goal without his patience and great passion for Science. It was a hard year for me and he did his best to help me and understand my situation. I am very thankful to have asked such a good person and scientist to be my supervisor.

Then, I would like to thanks also the team of CIWE lab of ETH, who was extremely kind and helpful. Thanks to Bärlocher Christoph, who built for me the wooden box for the experiment and the rest of the acquisition of the setup for the experiments. Thanks to Thomsen Henrik Rasmus and Aichele Johannes as well, who taught me how to use the LDV and discussed with me my technical problems.

Very fundamental was rule of The geology department of the university of Florence. Dr. Maestrelli and his team kept helping me also after the visit in Florence. Their contribution was crucial to understand the nature of the analogue modelling and it gave a great improvement to my project thesis.

Many other people should be thanks for the technical help. Besides, I would like to thanks my family, my parents, my aunts and Dario to have always been next to me, supporting me and loving me during this journey of two years of Master in Europe.

ETHZ University — Stella Cecchi
August 4, 2023

Table of Contents

Abstract v

Acknowledgements vii

Nomenclature xvii

Acronyms xvii

1 Introduction 1

1-1 Research Background . . . 1

1-2 Rationale for carrying out the research at CIWE[1] . . . 2

1-3 Thesis Outline . . . 2

2 Non-Linearity behaviour of the soft soil 5

2-1 The discovery of a non-linear elastic regime . . . 5

2-1-1 History of the most recent experiments on the non linearity . . . 6

3 Geometric and Dynamic Scaling 13

3-1 Geometric Scaling . . . 13

3-2 Geologic scaling: collaboration with the University of Florence . . . 14

3-2-1 Materials recommended and ultimately chosen . . . 15

3-3 Dynamic Scaling . . . 16

3-3-1 Elasticity Proportional Coefficient . . . 16

4 Building the Experiments 19

4-0-1 EXPERIMENT 1 & 2: 1 AND 2 LAYER MODELS . . . 20

Setup . . . 20

4-0-2 Acquisition . . . 21

5 Analysis of the Experiments **25**
5-1 Data Processing . . . 25
5-2 Results . . . 27
5-2-1 Results for the one layer model . . . 27
Velocity Analysis . . . 27
Wavefront analysis for the one layer model . . . 31
Conclusions for the processing of the one layer model . . . 32
Results for the two layer model . . . 35
Wavefront analysis for the two layer model . . . 37
Conclusions for the processing of the two layer model . . . 37
Interpretation . . . 37
5-2-2 EXPERIMENTS 3 & 4: NON LINEARITY OF THE 1 & 2 LAYER MODEL 41
Setup . . . 41
5-2-3 Acquisition . . . 41
5-2-4 Data Processing . . . 42
Non-linearity with respect to the Amplitudes . . . 42
Non-linearity with respect to the Voltage level (time-lag analysis) . . . 51
5-2-5 Results and interpretation of Experiment 3 and 4 . . . 52
Non-linearity with respect to the Amplitudes . . . 52
Non-linearity with respect to the Voltage level (time-lag analysis) . . . 57

6 Conclusions **59**

7 Outlook **61**

Bibliography **63**

A Additional comments on the computation of ΔI **65**

List of Figures

2-1 Fig.1 mentioned in the quote of [P. A. Johnson, 2005]. It shows the simplification of a non classic heterogeneous medium of soil with micro-grains inside. 7

2-2 Acquisition for my internship project at Geo2x. 3D wireless geophones were placed along a line. The source was the vibrator truck, called "MiniVib", which sweeped the input signal on the field from an offset position by changing frequencies and drive levels from 5% to 80% and downwards,too. 10

4-1 Pictures made during the building of the model for experiment 3. Step 1 was placing the clay bricks, step 2 was compacting the clay, step 3,4 and 5 show the last two sublayers. In the step 5, the clay was flattened with a sort of "rolling pin". Step 6 is the final result. 21

4-2 We had to spray some special product to increase the reflectivity of the clay to improve the signal. The blue robotic arm on the bottom right figure is LDV, the instrument we used to acquired the velocity as a substitute of the geophones. . . 22

4-3 Pictures made during the building of the model for experiment 4. Step 1 was placing a plastic folder to avoid the mixing of sand and clay. Step 2 was placing the sand next to the wooden box to work with that. Step 3 was putting the sand with a homogeneous distribution inside the box. Step 4 was flattening the sand. Then, the source was deployed in a non-symmetric position on the sand surface. Finally, step 6 is the acquisition of data. 23

5-1 Flowchart for experiment 1 26

5-2 Flowchart for experiment 2 26

5-3 Grid of interpolated points on the Clay from two different angles. 27

5-4 Slices of constant t, x, and y for the clay model. 28

5-5 Slices of constant t, x, and y for the sand-clay model. 28

5-6 Analysis of tx and ty slices for the clay grid. In green and red, the direct P- and S-wave traveltimes are shown. In white, the reflected P-wave traveltime is shown. 29

5-7 Analysis of SP Multiples of the Clay grid 30

5-8 Source wavefronts for the Clay grid. 31

5-9 Time slices of the clay grid. The Figure shows the waves as a response of the clay to the source input during time 32

5-10 Time slices of the sand grid. The Figure shows the waves as a response of the sand to the source input during time . . . 33
5-11 Analysis of direct and reflected wavefronts for the Sand grid (Later times). . . . 33
5-12 Analysis of direct and reflected wavefronts for the Sand grid (Earlier times). . . . 34
5-13 Analysis of direct and reflected wavefronts for the Clay grid . . . 34
5-14 Analysis of the reflection from the interface Sand . . . 36
5-15 Analysis of Clay events on the Sand-Clay vertical section . . . 37
5-16 Analysis of Clay events on the Sand-clay vertical section with highlights. The white rectangle shows the deformations of the amplitudes due to the reflection from the sand-clay interface. While the colored ellipses highlight events, of which we did not understand the nature . . . 38
5-17 Analysis of tx and ty slices for the sand grid. In green and red, the direct P- and S-wave traveltimes are shown. In white, the reflected P-wave traveltime is shown. 39
5-18 first part of the analysis of the wavefronts of the Clay grid . . . 39
5-19 Second part of the analysis of the wavefronts of the Clay grid . . . 40
5-20 Third part of the analysis of the wavefronts of the Clay grid . . . 40
5-21 Fourth part of the analysis of the wavefronts of the Clay grid . . . 41
5-22 Flowchart for Experiments 3 and 4 . . . 42
5-23 Normalized source and soil signals for (a) Two layer model and (b) One layer model. 43
5-24 Raw and normalized soil signals for (a) Clay model and (b) Sand-Clay model. . . . 44
5-25 Normalized source signals as images and waveforms for (a) Clay and (b) Sand-Clay. 44
5-26 Soils signals along the line for fixed voltage for (a) Clay and (b) Sand-Clay. . . . 45
5-27 Soils signals for all voltage levels for (a) Clay and (b) Sand-Clay. . . . 45
5-28 Linearity check of the amplitudes for (a) Clay and (b) Sand-Clay. . . . 45
5-29 Analysis of the residuals for (a) Clay and (b) Sand-Clay. . . . 46
5-30 ΔI and M matrices for the one layer model . . . 47
5-31 ΔI and M matrices for the two layer model . . . 47
5-32 Clay Model, Observed and Residual matrices (columns) for different p values (rows). 48
5-33 Sand-Clay Model, Observed & Residual matrices (cols) for varying p values (rows). 49
5-34 Summed residual value curves for (a) Clay and (b) Sand-Clay. . . . 50
5-35 Theoretical curves for the Clay model. . . . 51
5-36 Theoretical curves for the Sand-Clay model. . . . 52
5-37 Amplitudes for Drive levels Clay . . . 53
5-38 Amplitudes for Drive levels Sand . . . 54
5-39 Zoom and scaled Normilized Amplitudes for Drive levels of the Clay . . . 55
5-40 Zoom and scaled Normilized Amplitudes for Drive levels of the Sand . . . 56

A-1 The tapers we applied on the sand signal . . . 66
A-2 Source signal in 3 time windows, at the head, at the middle and at the tail of the whole signal . . . 67

A-3 Sand signal in 3 time windows, at the head, at the middle and at the tail of the whole signal 68
A-4 Zoom on one 68
A-5 Comparison of ΔI for four time windows, $tw_0 = [3050, 3090]; tw_1 = [3050, 3100]; tw_2 = [4950, 5000]; tw_3 = [6585, 6615]$. 69
A-6 Comparison of M for four time windows, $tw_0 = [3050, 3090]; tw_1 = [3050, 3100]; tw_2 = [4950, 5000]; tw_3 = [6585, 6615]$. 69

List of Tables

3-1 Table with the dimension and the characteristic parameters of the two layer model 14

4-1 Table with the most important acquisition parameters 24

5-1 Acquisition setup used in the non-linearity experiments 42

Acronyms

DUT Delft University of Technology

ETH Swiss Federal Institute of Technology

RWTH Aachen University

August 4, 2023

Chapter 1

Introduction

Since the end of the 90s, non-linearity in the response of the near surface has been studied, focusing on the possibility to characterize the soil through non-invasive field techniques, instead of through knowledge of site properties and laboratory measurements. In the first two decades of the new century, several teams tried to derive geotechnical parameters from active seismic data with quite interesting results (Boaga [2021]; Johnson [2009]). In fact, for the first time, it was possible to study the non-linear response of the shallowest soft soil to an acceleration greater than 1g generated by a shaker truck in situ, rather than through passive micro-tremors of natural origin.

This new geophysical method opened many questions and the purpose of my Master thesis was to answer some of them through a suitable combination of seismic processing of data acquired through geophysical field work and laboratory experiments. We would like to work on a bigger scale than the usual laboratory experiments on core sampling, but smaller than field work surveys. Thus, the research deals with intermediate-scale laboratory experiments, which offers the great advantages; on one side to be in a controlled environment with high resolution instruments, and on the other side to allow models really similar to reality.

1-1 Research Background

The idea for the project was born out of my 2022 summer internship with Geo2x Sa in Yverdon-les-Bains (Switzerland) and RealTimeSeismic (RTS), a seismic reflection processing outfit in Pau (France). I worked in the research and development department of Geo2x to develop an application of a new geophysical method that estimates some geotechnical parameters, such as damping factor, shear modulus, resonance frequency of the soil and quality factor from acquired field data. The reason was that those parameters are normally only estimated theoretically or through laboratory experiments. Geophysicists know well how to describe the properties of the soil when it behaves linearly, but not under condition of non-linearity. Thus, the purpose was to investigate the non-linear behaviour of the soil and derive some of its parameters.

I thus collaborated with Claudio Strobbia, owner and founder of RTS, to study non-linearity in the shear response of unconsolidated soft soil. Furthermore, in July 2022, I planned and directed a first test acquisition with Geo2x in Switzerland, while in August 2022 I read in, but did not process, the raw data. It turned out that by using a strong seismic source, such as the vibrator truck, we indeed induced non-linear behaviour in the soft soil overlying a high impedance layer in the shallow subsurface. Based on those observations, Geo2x and I were keen to continue the collaboration to research such non-linear behaviour of the soil and to estimate geotechnical parameters in the strong stress situation. However, because of the lack of time and inavailability of processing software, I could at that point not continue my research. Therefore, I contacted Dr. van Manen at ETH to propose a Master thesis project initially focusing on the estimation of shear strain in the shallow subsurface.

1-2 Rationale for carrying out the research at CIWE[1]

While working with a commercial geophysical company such as Geo2x offers many advantages such as availability of field data and access to equipment and instrumentation for large scale surveys, it quickly became apparent that such an approach has its downsides too: I tried analysing the field work data to understand the non linearity of the soil, but many issues cropped up. The field work happened in a real environment where the unknowns are more numerous than the knowns. Everything influences the survey, including for example the weather or the traffic. Studying a phenomenon of which very little is understood is incredibly hard to do in such an environment. One never knows if what one sees in the data is the response of the soil or if it is something else. Therefore, I thought delimiting the grade of difficulty of the problem could make the phenomenon much easier to analyse. In a neutral place, like a laboratory, one can control many starting parameters and focus only on the response signal. That is why I proposed to Dr. van Manen to build a model analogue of the field data created with Geo2x at CIWE[1], the ETH laboratory in Dübendorf. Furthermore, CIWE provides a sophisticated robotic arm with an instrument called an LDV[2] (from Polytec) that provides non-contact measurements of a medium's particle velocities. We believed the LDV could substitute the receivers used in the field and provide a much higher resolution and generally better results. The processing was carried out in MATLAB because the LDV software can output its data in a MATLAB format. Thus, this justified the idea of carrying out the research in the ETH laboratory and it shows promises for good results.

1-3 Thesis Outline

The aim of the Master thesis is thus to develop a method to estimate quantitatively and describe qualitatively the non linearity behaviour of soft soil in the laboratory. The research is divided in four parts:

1. First, the referenced field work surveys must be scaled to the intermediate laboratory scale, both geometrically and dynamically.

[1]CIWE: Centre for Immersive Wave Experimentation: https://eeg.ethz.ch/research/centre-immersive.html
[2]Laser Doppler Vibrometer

2. Second, the scale model must be built by hand in the laboratory.
3. Third, the influence of the finite size of the experimental domain (e.g., the boundary conditions of the box) on the recorded signals and the behaviour of the materials must be understood.
4. Finally, the geophysical active seismic must be re-created on the laboratory scale model and the non linearity behaviour of the soft soil studied.

The two main parts are to verify if we can correctly scale the field work to an intermediate scale and to see if we can observe the non linearity behaviour of the soft soil in our model. In addition, two extra results would be to understand the physics of such anomalous behaviour, and to figure out a method to classify the level of non linearity of a material and configuration. To the best of our knowledge, this kind of experiment has not been before and there have not been any physical definitions or classifications of the phenomena, yet. Therefore, scientifically speaking this research thesis is unique and first of its kind, because it could broaden the understanding of elastic materials and it would help to investigate the behaviour of the different type of materials under high forces, such as ground motions of earthquakes. Therefore, this research not only has pure scientific interest, but it could also bring novelties in the civil engineering regarding construction issues, as well as for modelling of natural catastrophes. In fact, the computed geotechnical parameters of the soil with non-linear behaviour may constrain initial boundaries and improve a local or regional earth models for forecasting.

Chapter 2

Non-Linearity behaviour of the soft soil

2-1 The discovery of a non-linear elastic regime

From the end of the twentieth century, different kinds of materials turned out to behave in a peculiar way when subjected to strong level of pressure. It was expected they behaved as classical elastic bodies, responding linearly to the stress, but it turned out their output signal had some non linear behaviours of unknown nature. It happened to be not a single case study. The non-linearity was noticed during both laboratory experiments with core sample of rocks and granular materials as well as during active seismic field works. The first field of science that discover this peculiar physical response of the crust of the earth was the geology. It was seen that earthquakes could trigger a non linear elastic dynamics on the crust. Many scientists were attracted by this unknown phenomenon, like geologists, mathematicians and geophysicists and physicists, and they tried to see the non linearity behaviour of several materials. The goal was to understand the nature of the non linearity, the cause that generate it and finding out if there was a correlation with the geology or chemistry of the stressed material. However, even if the subject was studied from many points of view with many experiments, the phenomena is still not totally understood. Currently, the physical causes are not characterised by a unique system of equations and scientists do not agree to a unique definition of the phenomenon. During the first decade of the twenty-first century, many correlations where found thanks to the improving of the technologies and so as many definitions were proposed, each coherent with the others but not totally complete.
The thesis research follow a thread in the history of non-linear soil behaviour woven primarily by the scientist A. P. Johnson. On our view, the contemporaneous specialist on the non linearity is Paul A. Johnson [1]. He dedicated great part of his career to understand how hard, soft, and granular materials react to a strong stress. He is specializing in Nonlinear and Disordered Systems and in Earthquake Source Mechanics. Being able to handle those two complementary field of science helped him to understand the physics of the NME [2] and

[1] Paul A. Johnson is a fellow Professor at American Physical Society from 2016. For more details see [Johnson]

[2] NME is for "Non linear Mesoscopic Elasticity

to correlate earthquake ground motions (P. A. Johnson [2005]) with non linearity behaviour of the soft unconsolidated soil (Johnson [2009]). His research was mainly based on interdisciplinary and scientific collaboration. In fact, what improved the characterization of the non linearity regime was studying it from different scientific fields, like geology, geophysics, chemistry, statics and so on.

2-1-1 History of the most recent experiments on the non linearity

Johnson has been collaborating with an interdisciplinary team in the last two decades. Firstly, in the 2004 with Alexander Sutin from Stevens Institute of Technology in New Jersey (P. A. Johnson [2005]). In their paper, they started form the classical theory and they distinguished two types of phenomenon: the Slow Dynamics (SD) and the Non Linear Fast Dynamics (NLFD). Their assumption was approximating the stressed body to a nonclassical material composed of grains connected by a "bond system", which causes the SD and ANFD. The main aims were to understand the generalization of SD and ANFD and to find correlation between them. They studied thousands of samples, selecting finally only seven of them, which were:

> "(...)gray iron, alumina ceramic, quartzite, cracked Pyrex, marble, sintered metal, and perovskite ceramic."[3]

They considered both the hysteresis and the visco-elasticity, but still it was not enough to completely define an equation for the non linearity. The next year, Johnson collaborated with Xiaoping Jia, from the Laboratoire de Physique des Mate´riaux Divise´s et des Interfaces of the Universite´ de Marne-la-Valle´(France), to study the earthquake triggering mechanism. In their paper ([Johnson and Jia, 2005]), they used an analogue model to study such enormous events like large earthquake in the small scale of the laboratory, scaling them from the continental crust to a granular media made of glass beads. The reason for that was to isolate the phenomenon in a controlled environment like the laboratory. There they could reduce the uncertainties and go to the hearth of the physics. For the first time was quantified the non linearity behaviour of the material by a parameter called β. It was proposed a second order linear expansion of the non-classical state equation of the dynamic stress that correlated it to the non linearity, as in equation (2-1) [4]:

$$\sigma_{dyn} = M\epsilon_{dyn}(1 + \beta * \epsilon_{dyn} + \delta * \epsilon_{dyn}^2 + ...) \tag{2-1}$$

If we assume the equation (2-1) to describe the correlation between the source input and the non linear response of the soil, we could say that the result of P. A. Johnson [2005] and Sutin was to isolated β, the first non-linearity parameter, but only later in time Johnson and Jia [2005] achieved to estimated also δ, the nonlinear second order parameter.
Apart for the strain characterization, another novelty brought by Johnson and Jia [2005] was quantifying the effects of the non linearity on the subject body. They saw the soil deformed

[3] [P. A. Johnson, 2005], abstract
[4] Johnson and Jia [2005], equation 1, page 873

under such strong ground motion and as a consequence, the soil changed its resonance frequency and Young Moduli. Therefore, they used the so-called "Resonant Method" to quantify the softing of the material[5].

By this analysis, It was understood that the composition of the material has a rule in the manifestation of the non linearity behaviour o the soil. They stated that the internal structure if composted of micro-grains triggers the non linearity response. They referred to a previous paper of almost ten years earlier, when Tencate and Shankland [J. A. Ten Cate, 1996] understood that the internal friction of the body components could had caused the phenomenon. [P. A. Johnson, 2005] explained the triggering mechanism of the non linearity behaviour by a simple model of the soil. The body could be seen as an heterogeneous medium of different size grains.

> "(...) The materials that exhibit ANFD and SD have in common a small volume of elastically soft constituents (e.g.,bonds in a sintered ceramic) where the SD and ANFD originate, distributed within a rigid matrix (e.g., grains in theceramic) as is shown in Fig. 1. We refer to this as the "hard/soft" paradigm. The soft portion of the material, the "bond system" is distributed throughout, but within a small fraction of the total volume, less than 1%. In cracked materials the bond system is localized.[7]"

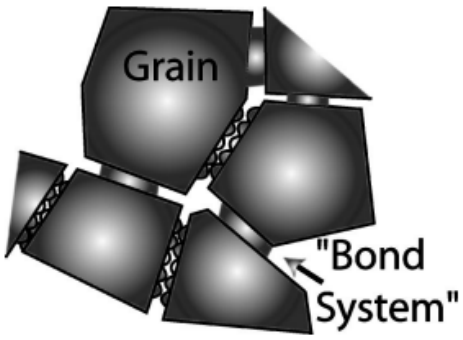

Figure 2-1: Fig.1 mentioned in the quote of [P. A. Johnson, 2005]. It shows the simplification of a non classic heterogeneous medium of soil with micro-grains inside.

You can think the triggering event of the non linearity behaviour of the soil as the resulting stretching of the bond system due to the grains collisions.

Leaving the classic mechanical physics, in 2004 V. Tournat and Castagnède [2004] [8] looked at the weak forces in the granular material with a probabilistic approach. Tournat's team

[5]The Resonant Method was already used in the 1996 by James Tencate and Thomas J. Shankland (J. A. Ten Cate [1996]). At the time, the evidence of a shift in the resonance curves respect to the frequency [6] was the empirical proof both of the correlation between frequency and source strain and of the existence of a non linearity behaviour in the soil (sandstone, in that specific case).

[7][P. A. Johnson, 2005],page 125

[8]from the Universite´ du Maine in France

considered the granular media as a ensembles of finite points that scatters with a certain stress and strain. They used the Hertz's non linearity of the contacts theory to relate the stress to the number of collisions and the strain. See equation (2-2) below:

$$\sigma = bn\epsilon^{2/3}H(\epsilon) \tag{2-2}$$

where σ is the stress, ϵ is the strain,b is a coefficent, n is the number of scatterings and H is the heavyside distribution.

In the paper [V. Tournat and Castagnède, 2004], they wanted to define a probability function that could describe the weak force distribution in the granular media. As in the previous papers, V. Tournat and Castagnède [2004] agreed with J. A. Ten Cate [1996] statement that the internal interaction of the micro grains in the material have a fundamental rule in the non linearity. Therefore, it seemed that granular materials were the best choice for doing experiment on the non linearity. In 2008, Thomas Brunet [9] collaborated with Jia and Johnson kept working on granular materials. In their paper,[Brunet and Johnson, 2008], they used a clapping model based on the Hertz contact theory, herniated by V. Tournat and Castagnède [2004]. At that time they faced the problem in a more empirical way, leaving all the mathematical assumptions. Brunet and Johnson [2008] focused on a dense granular packing with visco-elastic characteristics. The aim was to describe the wave demodulation in granular media. As quoted from the abstract of their paper:

> "(...) We evidence two distinct regimes of sound-matter interaction: reversible and irreversible, as a function of the ratio rs between dynamic strain and static one. In the reversible regime, the higher harmonics generated agree well with a mean-field model based on the Hertz contact theory, and the coefficient of nonlinearity beta deduced from the measured amplitude of second-harmonic is consistent with that deduced from the acoustoelastic measurement. Beyond a certain threshold ($rs >$ 3%), the interaction of sound wave with granular matter becomes irreversible, accompanied by a small compaction of the medium.[10]"

The state equation of the stress was re-proposed until the second order approximation with the addition of the viscoelastic contribution. They demonstrated by solving the equation using the Burger equation from plane waves that the Hertz theory reconstructs correctly the dynamics for low amplitudes, but it was incomplete to describe the internal dissipation mechanism in the granular media. To improve their experiment about non linear dynamics on the granular medium they suggested the following idea:

> "(..) the frictional dynamics at the grain contact level should be included [Nihei et al., 2000]. In studies of strong ground motion, it is clear that these hysteretic behaviours may play an important role; however, the effects of grain's shape and size dispersion as well as lower confining pressure condition should be considered in the future work.[11]".

[9] T. Brunet is from the Universite´ Paris-Est, in France
[10] Brunet and Johnson [2008], p. 1, abstract
[11] Brunet and Johnson [2008]; **?**]; Johnson [2009], p. 4

In the end, Brunet et al. opened a new research path to the future:

> "This work may provide a useful laboratory model for better understanding the large-scale field experiments such as nonlinear sediment response during strong ground motion.[12]"

The turning point for the non-linearity research was Z. Lawrence and Langston [2009][13], a paper published in 2004 few months later than Brunet and Johnson [2008] paper. It made do the jump from the small scale of the laboratory experiments to the big scale of the Geophysical field experiments. That paper is presented as a "prototype experiment" for future non-linear experiments:

> We present results from a prototype experiment in which we actively induce, observe, and quantify in situ nonlinear sediment response in the near surface.[14]

They used a vibrator truck to shake the experiment site surface and triggering Rayleigh waves. They observed anomalous response of the soil signal and they recommended in the end:

> Our results suggest that it may be possible to characterize nonlinear soil properties in situ using a noninvasive field technique.

In 2008 Johnson left the laboratory research for the bigger scale of the field experiments. He joined Lawrence in a Geophysics research, specifically an active seismic experiment, probably considering of particular interested the colleague's paper about the same subject. They re-proposed an active seismic field works with few accelerometers, in a short line configuration, where the source was located at its head. Johnson [2009] improved Z. Lawrence and Langston [2009] setup configuration, because it was proved there was no transversal variations in the horizontal plane respect to source direction. The great novelty brought by this paper was the introduction of a new geophysical method to study the non linearity of the soil in a big scale experiment[15].

[12] Brunet and Johnson [2008]; **?**]; Johnson [2009], p. 4

[13] Dr. Lawrence is part of Cooperative Institute for Research in Environmental Sciences (CIRES), works at the University of Colorado Boulder, Boulder, CO, USA; and it is memember of NOAA Physical Sciences Laboratory (PSL). For more details see Lawrence

[14] [Lawrence and Brackman, 2008], abstract

[15] For further information about the goals achieve by Johnson [2009], we quote a part of the paper abstract.

> Here we introduce a new method for in situ characterization of the nonlinear behavior of a natural soil formation using measurements obtained immediately adjacent to a large vibrator source. To our knowledge, we are the first group to propose and test such an approach. Employing a large, surface vibrator as a source, we measure the nonlinear behavior of the soil by incrementally increasing the source amplitude over a range of frequencies and monitoring changes in the output spectra. We apply a homodyne algorithm for measuring spectral amplitudes, which provides robust signal-to-noise ratios at the frequencies of interest. Spectral ratios are computed between the receivers and the source as well as receiver pairs located in an array adjacent to the source, providing the means to separate source and near-source non-linearity from pervasive non-linearity in the soil column. We find clear evidence of non-linearity in significant decreases in the frequency of peak spectral ratios, corresponding to material softening with amplitude, observed across the arrays the source amplitude is increased. The observed peak shifts are consistent with laboratory measurements of soil non linearity.[16]

After more than ten years, Boaga [2021] presented a geophysics experiment to study the non-linearity. An active seismic setup was used, triggered by a Vibrator truck, which did a sweep through a range of frequencies for different drive levels. They investigated the surface in two ways. Firstly, the anomalous phenomena was correlated respect to the estimated induced strain and secondly, by looking at the Rayleigh waves behaviour. They observed the resonance frequency of the top layer changed and it experienced softening of the soil[17]. The research pointed out the possible dependence of the non linearity response of the soil to the top layer internal structural characteristics. What is clear is that this research is based on Lawrence and Brackman [2008] for the used of the Rayleigh waves and Johnson [2009] for the setup and estimation of the strain in situ. Boaga [2021]'s research is the first paper to show a way to reconstruct the shear modulus curve over the strain of the specific field[18]. That was what caught the attention of Geo2X Sa company (Yverdon-les-bains, Switzerland). That is how I started to work on the non linearity behaviour of the soil (for other information look at 1 or to [Cecchi, 2022]).

Figure 2-2: Acquisition for my internship project at Geo2x. 3D wireless geophones were placed along a line. The source was the vibrator truck, called "MiniVib", which sweeped the input signal on the field from an offset position by changing frequencies and drive levels from 5% to 80% and downwards,too.

A part for the acquisition, I had to move to France, in Pau, to use powerful softwares to

[17]The change in Young Modulus was already observed by previous papers, [J. A. Ten Cate, 1996],[Brunet and Johnson, 2008],[V. Tournat and Castagnède, 2004]

[18]usually the shear modulus is not computed in situ but by laboratory estimations. Any methods to estimate the strain in the field experiments have been proposed yet.

process the data. I worked for a month at Claudio Strobbia's company, RealTimeSeismic [19]. There, I look at the raw data and we showed the non linearity effect on the signal, but I could not process the data and neither compute the shear strain, because of the lack of time, because my internship ended with the starting of the second year of Master. I liked the project so much that I did not want to let it incomplete and I decided to continue the research with my Master Thesis at the CIWE laboratory of ETHZ University in Zurich (Switzerland).

[19] RealTimeSeismic (RST) is a private reflection seismology preccessing company in Pau, France

Chapter 3

Geometric and Dynamic Scaling

The thesis project would like to recreate in the laboratory a field experiment similar to Boaga [2021]. This means all the geometrical characteristics of the setup and the physical quantities have to be scaled to a smaller scale. Generally, a field experiment is in a particular environment characterized by the geology of the site. The geophysical method employed should be such that it recreates the stress regime that the soil was subject to. Thus, also, the type of source must be considered, how it works and how its signal spreads through the subsurface. Therefore, when one scales an experiment the first thing to worry about is the geometry of the setup, in other words, the so-called "geometrical scaling".

Apart from the static state of the experiment, it is crucial to focus on what happens during the triggering of the input signal. For example, a geophysical vibroseis survey stresses the soil with a certain force and strain level and for that specific trigger the subsurface behaves in the way that we want to study. Therefore, being aware of the physical quantities involved in the "dynamic state" is fundamental to correctly recreate the experiment on a different scale. What we call dynamic scaling is the process of proportionally scaling the physical quantities of the reference experiment in a non-static state to the desired new scale.

Thus, the physics of the scaled problem is coherent and, most importantly, the scaled problem behaves in the way we want to study. Contrarily, a not well-scaled experiment could provide non-trustworthy data, and, in the worst case, produce other phenomena which we do not want to study. In order to achieve our goal to study the non linearity behaviour of the soft soil, the geometry and the dynamic quantities must be scaled correctly.

3-1 Geometric Scaling

The Boaga [2021] and Johnson [2009] papers both present active seismic surveys, using a vibrator truck as a source. The geology of the site is simplified as a two layer model of infinite width and length. For Boaga [2021], the first layer is a sand deposit overlying a second layer sandstone formation. The layers are thin, e.g., 4 meter each. On the other hand, the survey of Johnson [2009] has a thicker first layer of 11 m, consisting of a young and unconsolidated

layer	clay	sand
thickness (m)	0.45	0.12
density (kg/m^3)	2000	1600
diameter grain (mm)	0	0-0.22

Table 3-1: Table with the dimension and the characteristic parameters of the two layer model

point bar sediment overlying a soft shale of unknown depth (due to the assumption on the model that the second layer is semi-infinite). The main starting hypothesis for non linearity to occur is that a soft unconsolidated layer overlies a hard bedrock; a condition which was met in both papers (but also in others, see chapter 2). Thus, the second layer must be denser and more compact then the first, which has the peculiarity of containing micro grains of different sizes randomly distributed. Regarding the acquisition setup, Boaga [2021] used 61 geophones with 2 m spacing. So, a line length of around 120 m. We do not consider the acquisition setup of Johnson [2009] because it was a very short line, not really helpful for our experiment.

To summarize: the theoretical reference field experiment consists of active seismic along a line of around 100 m length, using around 61 3C-geophones. On the geological side, both sites were made of two sublayers: e.g., sand deposits and sandstone. The shallowest layer was unconsolidated, less compact, and less dense than the second layer, which behaves like a bedrock. The shallow layer has micro grains inside. The volume is semi-infinite on the depth and it is wide and long (e.g., 100 m).

The scale chosen, between, respectively, the laboratory experiment and field work, is thus 1:100. The geometry of the experiment should respect this proportion to have the correct geometric scaling. Fortunately, we did not have to acquire the data with 3C-geophones, which would have been difficult to scale, but we could use the LDV, which also measures three velocity components. Apart from that, the order of the number of points acquired along any particular dimension was the same: $\sim$60. Instead of having a practically unlimited volume as for the field works, we delimited the volume to a hand-made wooden box. The rectangular wooden profile of the box was approximately 1 m long and wide, so that 1 m of the laboratory space corresponds to 100 m of the field acquisition space. The first layer is made of sand with grains of diameter between 0 and 0.22 mm, while the second layer is clay. The density and the compactness level of the clay are greater than the sand. Note that we had to work with a finite volume much smaller than the field volume of the reference surveys, so we chose a thickness of the harder second layer sufficiently greater than the thickness of the upper layer. Hence, the shallow layer is so much smaller than the deeper one such that it is comparable to the field experiment. Therefore, we chose to make the lower layer almost 50 cm thick while the first sand layer had a thickness of approximately one quarter of it, i.e., around 12 cm.

A large part of the research was devoted to deciding the best materials for the sublayers; even more than to understanding how to scale the setup of the experiment.

3-2 Geologic scaling: collaboration with the University of Florence

As for the geometric scaling, choosing the material for the model is crucial both to verify the non linearity regime and to be able to compare the results with a reference experiment on

a bigger scale. To recap: our wish is to compare our data with the results of Boaga [2021] and Z. Lawrence and Langston [2009] (whose experiment Johnson [2009] mostly improved). As they underlined in their papers, there is the hypothesis that the non linearity is due to the internal friction of the micro grains in a soft unconsolidated material overlying a harder material. Since we wanted to be sure to reproduce the non linearity, the challenge was to find the best scale material for that.

Reading papers on previous lab tests investigating non linearity was helpful to broaden our knowledge of that field, but not enough for selecting a material (particularly because previous laboratory experiments have all been on the core/micro scale). What transpired from meetings at ETH with scientists from the rock physics laboratory was that this kind of scaling is mainly used in geology. Tectonics dynamics and other mechanisms in the crust took thousands (if not millions) of years to happens and nevertheless a geological field exists to study them by recreating the phenomena in the laboratory and on the human time scale.

Fortunately, a team of the University of Florence (UoF) visited ETH shortly before the meeting about my thesis project. This research group works on so-called "Geological Analogue Modelling". Thus, we thought a collaboration with them could help us to choose the correct material. I contacted Dr. Daniele Maestrelli, researcher of the geological department of the UoF. He and his team welcomed me in Florence for an open day in their laboratory. I spent a full day in the department, where they introduced me to their techniques of analogue modelling and I had an intensive course about geometrical and dynamic scaling as used by geologists. I even built a rift geological analogue model with one of their PhD students.

Prof. Marco Bonini and Prof. Giacomo Corti welcomed me in the laboratory, and the showed to me the main device used for this kind of analogue modeling studies: the centrifuge. Prof. Bonini created the laboratory and brought the centrifuge back from Sweden at the end of the '90. Sweden was the first country to produce such machine. The centrifuge has two small baskets where you can place the analogue models and make them run at high acceleration levels, that can be multiples of the gravity. The centrifuge controls the temperature and other environmental conditions as well. The size of their geological analogue models is small, on the order of centimeters, but they can recreate with them what the crust did in millions of years in a very short period of time. It is a powerful machine and a highly interesting method.

The visit thus was productive, and I got recommendations for my thesis, new papers, and books to read about the subject, but mostly I saw with my eye how geological analogue models are built. Seeing how create sublayers of the analogue model, how to place the material in the container, how it reacts to the centrifuge force and touch the sands they used, opened my eyes on the concept of scaling. Each material has different qualities and their compactness, viscosity or grain sizes influence drastically the experiment. In their laboratory, the have a wide range of media, from highly plastic materials to very unconsolidated and quartz sands. Something I have never experienced before.

3-2-1 Materials recommended and ultimately chosen

The k-feldspatic sand FS900S was the only material considered useful for our experiment that they had present in their laboratory. Its grains were really fine, more cohesive[1] than other

[1]The concept of cohesion plays an important role in geologic analogue modeling as it xyz...

quartz sands, but it has some disadvantages. The grains have the same diameter, and they are uniformly distributed throughout the volume. Those characteristics are the opposite of what we look for. We would like a random distribution of grains with different diameter sizes. Moreover, the level of compaction is too low and it may affect the response to the signal. In reality, a field of sand deposit is more plastic due to the presence of other materials and more dense. It is questionable whether they could be scaled with such fine sands. In addition, the k-feldspatic sands are produced in Germany only sold in large quantities (e.g., 1500 kg) and not in the small quantities we need for the thesis project. Time is an important variable to consider, too. The thesis research has to be done in few months, so it is crucial to choose a material available in the market. Therefore, a suggestion from Dr. Maestrelli was to consider materials such as chalk and clay for the top and bottom layers of the analogue model.

The main learning from this experience was that not only we have to scale the geometry of the set up, but also the forces. The forces acting on our model are dependent on the material chosen, too. Therefore, we need a material with a similar structure as the field experiment of Boaga [2021]. The first layer was a deposit of sand with grains of random geometry, thus, on our view, the best fit was the sand used in the playing ground for children. It is plastic, compact, and most important, with random distributed grains of diameter in the range of millimetres. As for the bottom layer, we settled on the idea of clay, because it can act like a bedrock for a softer and less compact material like sand. The clay used is the pottery one that comes in bricks. It is easy to handle and shape. We bought it from a specialist manufacturer/producer of clay for artists.

The density of the clay is 2000 kg/m^3 whereas the density of the sand is 1600 kg/m^3, the thickness of the clay layer is approximately 45 cm while the thickness of the sand is almost 12 cm. The total thickness of the two materials in the box is approximately 57 cm.

3-3 Dynamic Scaling

Despite the fascinating science and results that can be achieved with it, geologic scaling is not adequate for geophysical experiments. Geological analogue models study the response of a large volume of crust and mantle of the Earth under the force of gravity over a long period. The body is in a quasi-static state and the only acting force is gravity. In active seismic, the field is in a static state until the experiment begins. The field experiences the stress of the source and its response is transduced into displacements. The dynamic scaling in geology takes into consideration the potential field of the gravity force, while in this geophysical experiment we can ignore the gravity, because it has no effect towards changing the body; the wave time scale is incomparably short relative to the geological time scale. But we must consider the source force. The same force and stress and strain in the field work of Boaga [2021] must be re-created in this thesis project. Thus, the dynamic scaling's main aim is to check that force proportionalities are respected.

3-3-1 Elasticity Proportional Coefficient

From previous papers (see also chapter 2), it is known that soft soil behaves non linearly when the source strain exceeds 10^{-6}. We want to work with a strain in this range to be

sure we see the non linearity. How do we ensure the dynamic scaling then? We assumed the analogue model is an elastic body, because it deforms and experiences displacements of the surface during the source stress but then it goes back to the original state. Under this condition, Hubbert [1937] stated that a well scaled analogue model should have the same value of the ratio stress/strain of the real phenomena. The ratio takes the name of "Elasticity Proportional Coefficient" (EPC). As a consequence, the EPC of our model should equal the EPC of Boaga [2021]. If they are, then the dynamic scaling is correct, in addition to the geometric scaling, and we can use the data from our experiment to study the non linearity.

Mathematically, the elasticity proportional coefficient, C, is defined as follows:

$$C = \text{Stress/Strain} \tag{3-1}$$

$$Stress = \text{Force/Superficial Area} \tag{3-2}$$

The force can be measured on the source (as is routinely done for vibroseis with the help of accelerometers[2]) and the area considered can be the taken to be the baseplate of the vibrator where it sweeps on the ground. For the piezoelectric source it is exactly its area, because it is placed directly on the sand, whereas the force could be computed from the piezo-electric constitutive equations. Such a computation should work theoretically, however is not possible to do for us, for two main reasons:

1. Firstly, it would be out of the scope of the thesis to compare the analogue model with another newly constructed field survey.

2. Secondly, the idea for our experiment came from a mix of experimental setups from previous paper about non linearity, but it does not refer specifically to one of them. Thus, we cannot compare the coefficient to anything.

In addition to those points, estimating the stress and the strain is also a time-consuming task that with the limited time available for the thesis is definitively out of scope. We leave the task of creating the same experiment on the field scale and the laboratory scale and verifying the dynamic scaling to future researchers interested in the non linearity topic.

Thus, a valid question is: how did you reach the force or strain level required to reach the non linearity if you did not mathematically derive the values to use? The answer is by trying. In science, most of the time it is not the theory that drives the experiment, but it is the experiments that give hints to scientists to understand unknown phenomena. Less poetically and more practically, what we did was we experimented with different source setups and analysed the responses. We read that field works of Boaga [2021] and Lawrence and Brackman [2008] used a driving force of 10^3 N. So, we chose a piezoelectric source with the same order of magnitude and a scaled diameter. We changed frequencies, range of voltages, type of impulse, etc., until we found what we wanted: a hint of non linearity response in the soil signal.

In conclusion, for a variety of reasons, it was not possible to realize a complete dynamic scaling of the analogue model. We did not have a precise large scale experiment to which to compare to and we did not have time for a second project for the estimation of the shear

[2]In particular, there is the concept of (Fundamental) Ground Force, which is the force exerted by the vibroseis less distortion. This is the desirable energy produced by the vibroseis and ultimately transferred into the ground.

strain. But, we would like to recommend to focus on the check of the dynamic scaling from a field survey to an intermediate scale experiment in the future. That could bring novelties to the field of the strain estimation, as well. In fact, the big problem is quantifying the strain in the situ rather that in the laboratory, because there the situation is more uncontrolled.

One idea that we suggest is to use fibre optics with an interrogator to directly estimate the strain both in the field and in the laboratory. Obviously, the fibre dimension must be proportional to the scale, thus longer and thicker for the field. Considering Sollberger and Robertsson [2020] and Schmelzbach and Robertsson [2018] recently started projects regarding shear strain estimation, the geometry of the optical fibre has an important effect, too. Perhaps basing the future research on their latest papers could help the future projects. In addition, another point would be to check the if EPC is the same for both experiments or if the non-linearity is influenced by it as well.

Chapter 4

Building the Experiments

The main part of the thesis consists of a set of experiments that attempted to recreate a seismic survey in the small scale of the laboratory. The purpose was to see if we can observe non linear behaviour for one and two layer models. The configurations were mainly based on the field surveys of Boaga [2021] and Johnson [2009]. We would like to stress the uniqueness of these experiments: as far as we know, they are the first intermediate-scale experiments investigating non-linearity by creating one and two layer geophysical analogue models.

The first step was to physically create the analogue model. As mentioned in Chapter 3, we would like to work on an superficial area of (1x1) m and total depth of around 60 cm. The laboratory technician kindly built a wooden box of (1x1x1) m not closed on the top and the bottom. The lateral faces of the box were placed on a plastic pallet, so that the base of structure was approximately 16 cm above the ground. We then distributed the bricks of clay (see Chapter 3) horizontally and created 5 levels of clay. For each level we compacted the material by pressing with hands and feet in such a way that the most of the air vacated the spaces between the bricks and together they formed a unique sublayer. When each layer was sufficiently compacted, we distributed the clay on the surface as equally as possible, to have a horizontal plane. In particular, we were careful to do this for the last clay layer. The superficial face of the clay had to be as flat as possible. To make it flat, I copied the technique shown to me during my stay in Florence.

As mentioned in section 3-1, I observed the construction of an analogue geological model in the geological laboratory of the University of Florence. The scientists there were working on a small scale of 20x10x5 cm and were using very fine sands. They spread the sand with a small, smooth-edged, toothless wooden rake. Step by step, the sand was spread all across the surface and when ready, new sand was added. In the end, for the final surface, they placed a plastic sheet over the sand and, with a small rolling pin, they finished their geological model.

So, I imitated their technique and used a plastic cylinder of larger diameter (such as the one used to transport water or electric cables) as a rolling pin. But, it turned out it was much more challenging to use this technique with the clay, because it is a very compact material and one needs to push with all their body weight to flatten it. Moreover, the “rolling pin”

was significantly shorter than the side-lengths of the box and the distribution of the clay was not as perfect as hoped for. The same process was repeated for the sand, and, obviously, it was much easier, because it is much less cohesive than the clay. On that occasion, we were able to use the tool to clean car windows to flatten the sand and it worked fairly well. To be sure, we also used a spirit level to check if it was horizontal and were pleased with the result. To measure if the source could have buried itself during the sweeping due to compaction we suspended a cord with a weight next to the source with the bottom of the weight level with the top of the source. We were mainly worried that this could happen for the sand, but it did not happen, at least not observably. The fact that the clay surface was not completely flat also was not an issue, because the LDV can measure the elevation of the points. Therefore, we could plot a map of the points in 3D and before processing, we interpolated the coordinates.

On the other hand, for the set up of the source, we had to do many preliminary tests before reaching the final setup. In the beginning, it was more a matter of knowing the material we working with. For instance, when we familiarized ourselves with the source, we learnt how the piezoelectric actuator material reacts to certain driving frequencies or voltages levels, or which base plate we should use over the surface such that the source does not bury itself into the material. Further, we wanted to see if the wooden box influences or interferes with the acquired data, for example, if the waves scatter from the sides of the box or if they scatter from the ground and then back to the LDV receivers. It turns out that there was no big influence of the bottom of the box (i.e., the plastic pallet) on the data. Perhaps the dimension of the box with respect to the LDV measurement grid was much larger such that the waves were already significantly attenuated as they reached the bottom of the clay and therefore did not reach the floor. We noted that between the end of the clay layer and the ground there is approximately 16 cm of air. Finally, the side walls of the box had an effect in the data, but we will talk in more detail about that later, when we will describe the mirror source wavefront analysis.

Having acquired all that new knowledge, we could then focus on the real experiments. In total, four experiments were carried out for this thesis's project: two to characterise the clay model and the two layer model (sand and clay), and two to study of the non linearity for the clay, one layer model, and for the two layer model.

4-0-1 EXPERIMENT 1 & 2: 1 AND 2 LAYER MODELS

Setup

The set up used in the laboratory was the same for both experiments:

- Wooden box filled with the clay to a height of 45 cm,
  with sublayers of around 10 cm thickness each
- Piezoelectric source
- LDV
- Generator

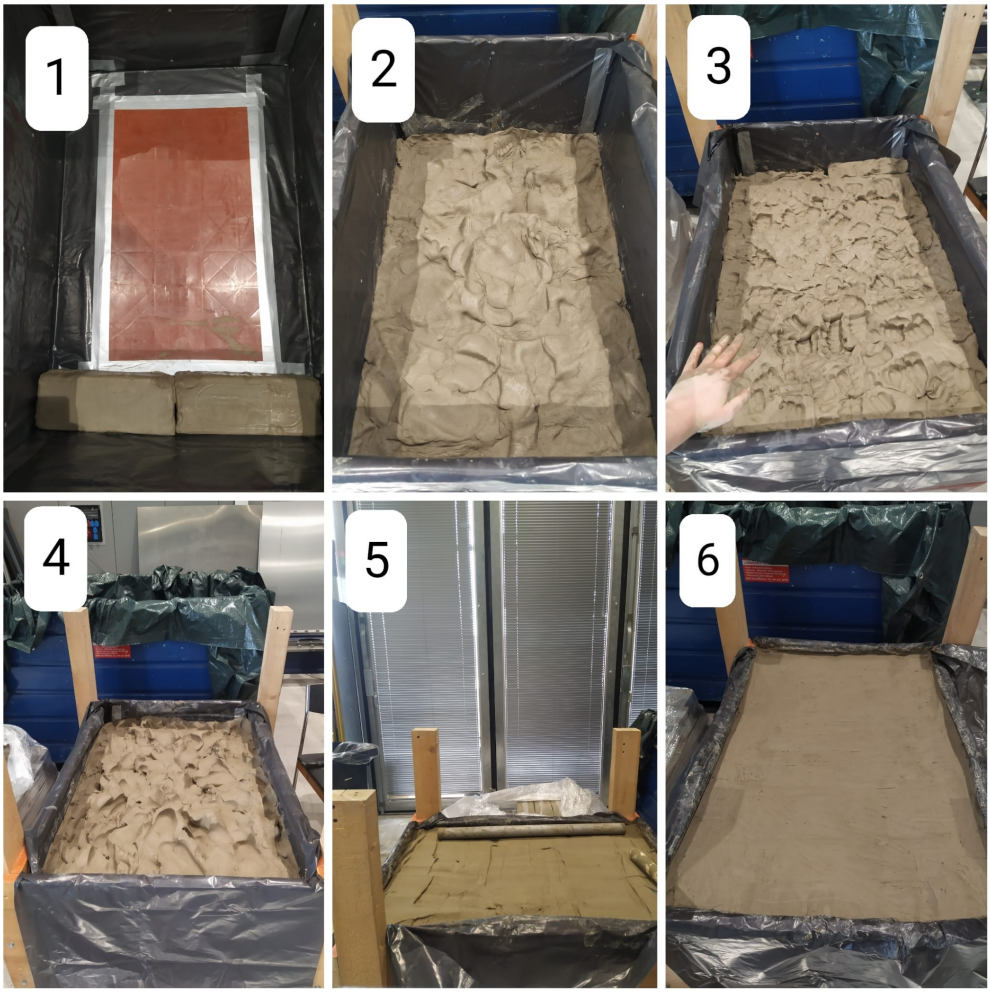

Figure 4-1: Pictures made during the building of the model for experiment 3. Step 1 was placing the clay bricks, step 2 was compacting the clay, step 3,4 and 5 show the last two sublayers. In the step 5, the clay was flattened with a sort of "rolling pin". Step 6 is the final result.

- Amplifier

4-0-2 Acquisition

The source was a pulse signal induced by the generator but triggered by the LDV. The points acquired were 845 in a rectangular structure with a corner originating in the centre of the source. The source was placed at 15.3 cm away from the side of the box along the y axis and 29 cm from the side along the x axis. Thus, the source was in an asymmetric position with respect to the xy plane, with a shorter length for the x side. The parameters used for the experiments are in Table 4-1.

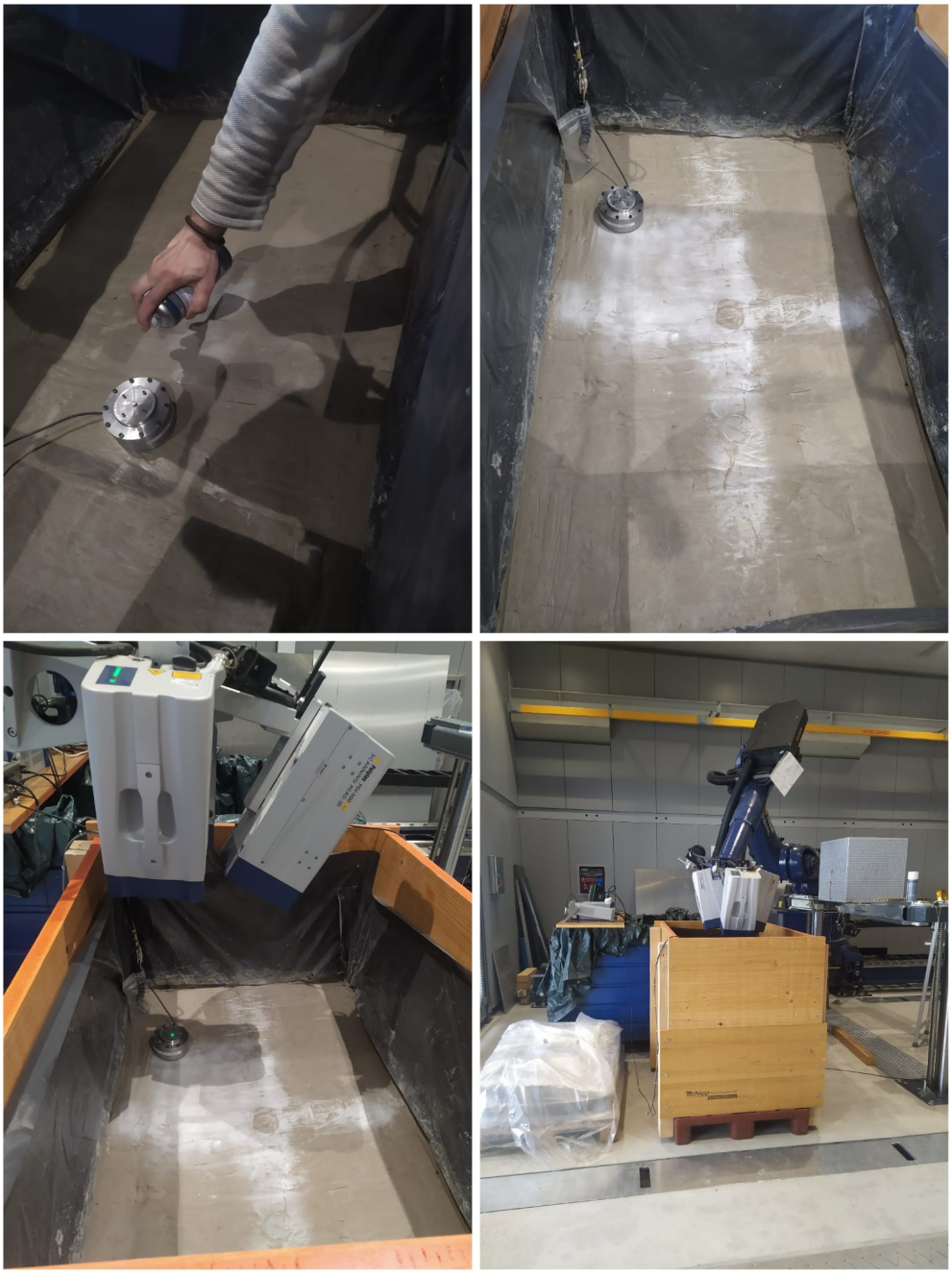

Figure 4-2: We had to spray some special product to increase the reflectivity of the clay to improve the signal. The blue robotic arm on the bottom right figure is LDV, the instrument we used to acquired the velocity as a substitute of the geophones.

Figure 4-3: Pictures made during the building of the model for experiment 4. Step 1 was placing a plastic folder to avoid the mixing of sand and clay. Step 2 was placing the sand next to the wooden box to work with that. Step 3 was putting the sand with a homogeneous distribution inside the box. Step 4 was flattening the sand. Then, the source was deployed in a non-symmetric position on the sand surface. Finally, step 6 is the acquisition of data.

	generator		LDV
Amplitude High	500 mV_{pp}	n points	845
Voffset Low	250 mVdc	n stack	200
Width Duty	400 mus	sampl. f	100 kHz
Edge Time	100	samples	4800
Frequency period	100000	delay in t	50 ms
		trigger input	internal
	source		
signal	pulse		
type of input	burst		
n cycles	1		
trigger	external		
direction trigger	raising		

Table 4-1: Table with the most important acquisition parameters

Chapter 5

Analysis of the Experiments

5-1 Data Processing

We start by analysing the LDV data recorded for the impulsive source signals. In the next chapter we analyse the data acquired with the frequency swept source signals. The processing of the data was done using MATLAB. Two scripts were created to process the data from the clay model and the two layer model, respectively. The goals of these scripts were twofold:

1. Firstly, to identify the wave propagation velocities of the clay and of the sand, to derive, if possible, the thicknesses of the sublayers of the clay in the one layer model and the depth of the sand-clay interface in the two layer model.
2. Secondly, to identify the influence of the model and the box structure on the output signal, or in other words, how the material models the waves and their wavefronts.

Both pieces of information help with the interpretation of subsequent experiments to separate patterns related to the material and the box structure from the nonlinearity effects.

Figure 5-1 and 5-2 clearly display the steps of the MATLAB scripts. To summarise, it divides in two types of analyses: Velocity Analysis and Wavefront Analysis. The idea of the former is to derive the P- and S-wave velocities of the clay and sand by plotting slices of constant t, x, and y through the 3D data volume and modeling the arrival times of specific events. I derived the P-wave velocity of the hyperbolic event, which is the reflection from the bottom of the clay for the one layer model and the reflection from the sand-clay interface for the two layer model. Note that the velocities found for the clay on the one layer model are required as inputs for the final analysis of the waves on the two layers model. Thus, I estimated the heights of the clay and the sand layer. While, regarding the wavefront analysis, I changed the coordinate systems to the coordinate system of the sources and I plotted wavefronts over the time slices of the recorded signals for the real and mirror sources. This was done to identify the direct wave from the source and from the mirror source (i.e., the reflection from the wooden interface). At the end of the processing, I include an annotated picture of how the two layer model behaves when stressed by the piezoelectric source.

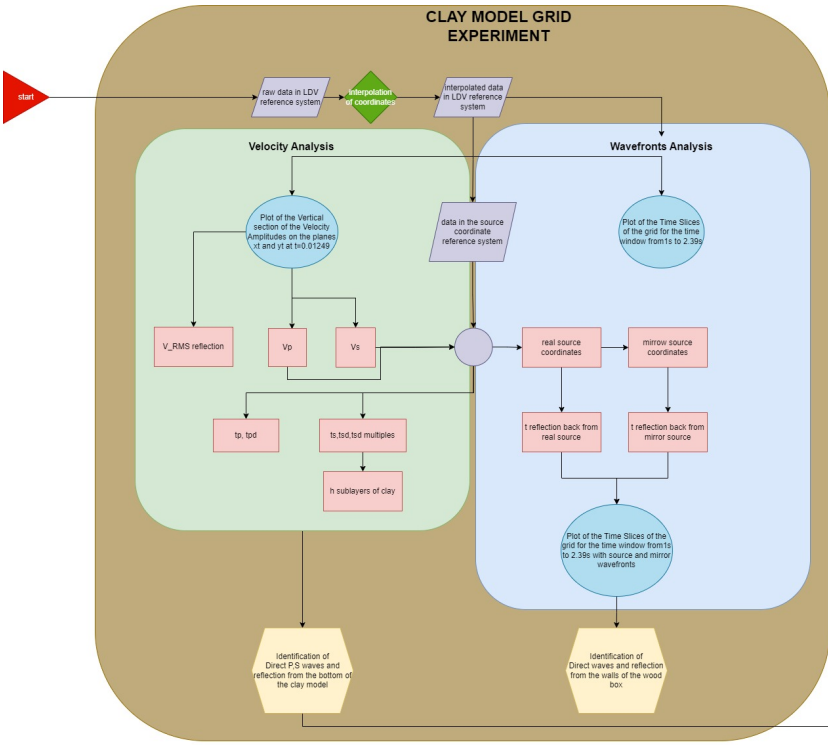

Figure 5-1: Flowchart for experiment 1

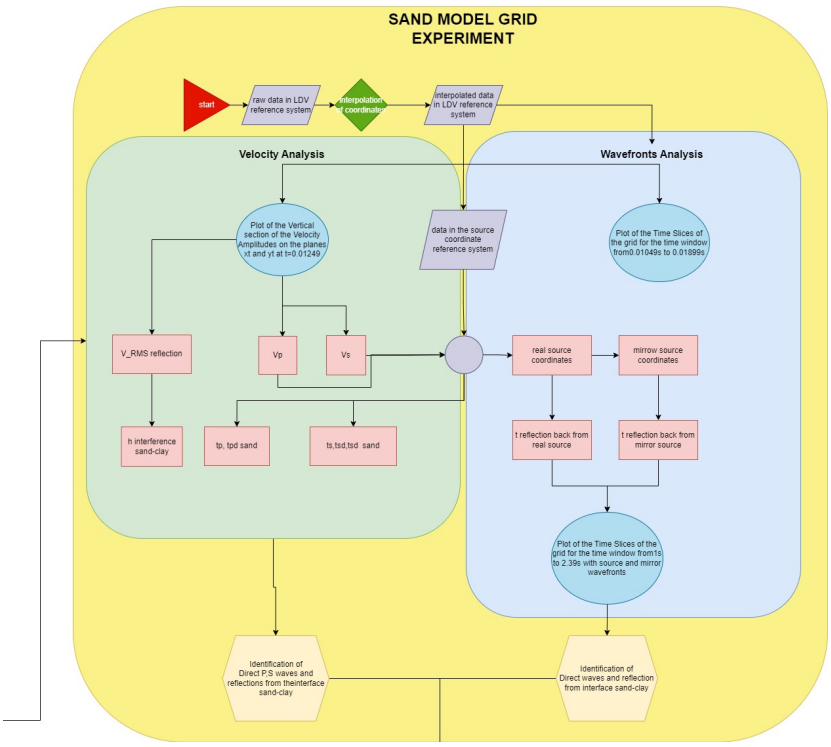

Figure 5-2: Flowchart for experiment 2

5-2 Results

5-2-1 Results for the one layer model

Velocity Analysis

The first step is to visualise the elevation of the grid points available from the LDV measurements in 3D space. As visible in Figure 5-3, the acquisition surface was not flat at all.

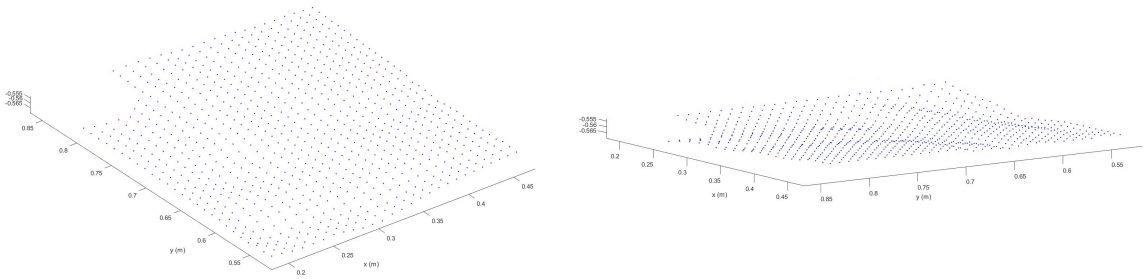

Figure 5-3: Grid of interpolated points on the Clay from two different angles.

The issue was that the high degree of compaction of the clay made it difficult to shape the surface as wished. Fortunately, thanks to the 3D-3C LDV measurements, it was not a problem for our experiments, provided it was taken into account in the processing. In fact, before doing any manipulations of the raw data, I interpolated them in order to have a better distribution in the horizontal plane. Note that the source created a blind corner in the grid, due to the radius of the source of 2 cm[1]. Based on the 3D LDV videos of the propagation of the wavefronts for experiments 1 and 2, a specific time (t=0.01249 s) was chosen for which the direct waves already propagated beyond the scan grid but for which some interference of unclear origin was noticed for experiment 2.

In Figure 5-5, the time slice clearly shows two spots. These are named P_1 and P_2 for simplicity. We will try to explain their existence in the following. Hence, a slice at that particular time was considered, in combination with slices of the seismic acquisition on the yt and xt planes. Studying Figure 5-4, I recognized what appear to be the direct P- and S-waves and computed their velocities with the help of the Matlab function *ginput*, picking the two points defining the slope directly from the plot. The equation for the velocity of a direct wave is as follows:

$$v = (x_2 - x_1)/(t_2 - t_1), \tag{5-1}$$

where (t_1, x_1) and (t_2, x_2) are the points defining the extremes of the wave considered[2].

The so estimated direct wave velocities in the clay are: $V_P = 70\ m/s; V_S = 21\ m/s$.

[1] The idea was to have two edges of the scan grid coincide with lines through the center of the source.

[2] It is of course not necessary to pick the points at the extremes. However, in general, the accuracy of the estimated velocities will be improved if points at the extremes are chosen since the picking error gets relatively smaller the larger space and time intervals are considered.

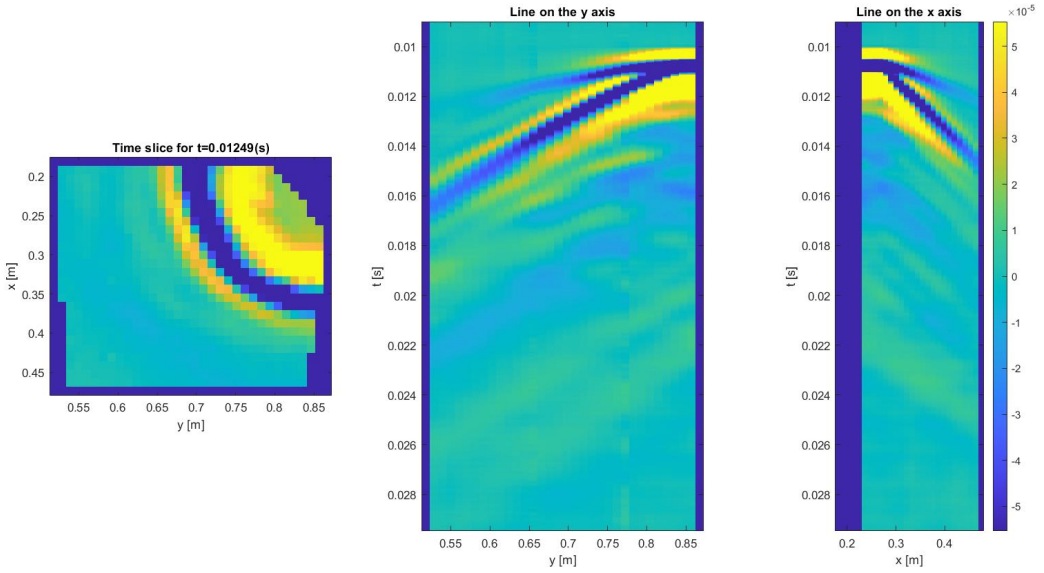

Figure 5-4: Slices of constant t, x, and y for the clay model.

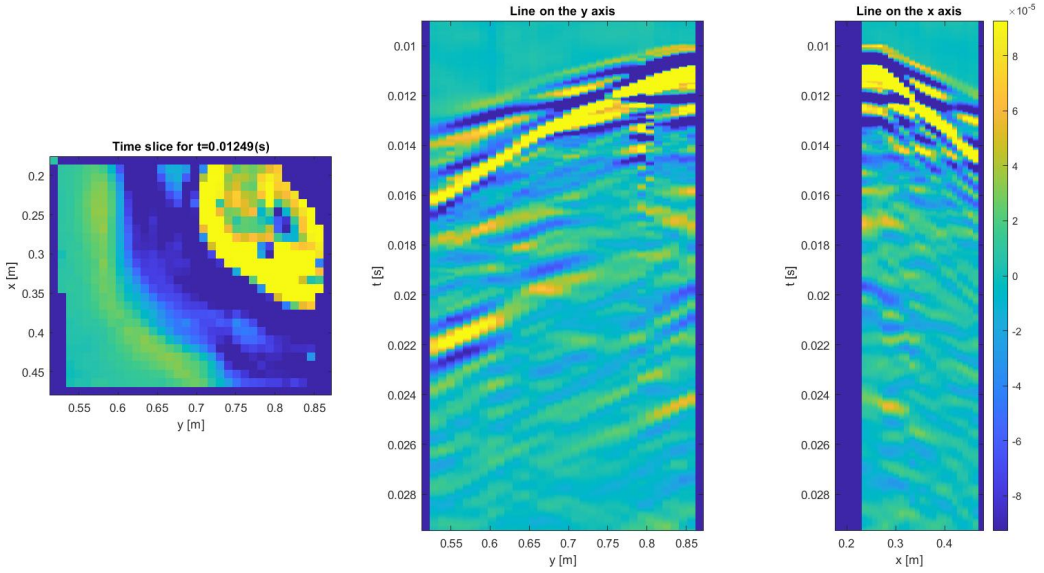

Figure 5-5: Slices of constant t, x, and y for the sand-clay model.

To check the credibility of these values, I plotted the predicted arrival times for the direct P- and S-wave and the reflected P wave over the ty and tx slices using the following equations:

$$t^P_{direct} = t_0 + y/V_P, \quad \text{and} \tag{5-2}$$
$$t^S_{direct} = t_0 + y/V_S, \tag{5-3}$$

where t_0 is the measured source actuation time, found by picking the maximum of the signal

measured on the source with the LDV, and y is the distance from the source. And,

$$t^P_{reflected} = t_0 + dist_y/V_P, \quad \text{and} \tag{5-4}$$
$$t^S_{reflected} = t_0 + dist_y/V_S, \tag{5-5}$$

where $dist_y$ is the two-way propagation distance of the reflected wave:

$$dist_y = \sqrt{(2d)^2 + y^2}, \tag{5-6}$$

and $d = 0.40\ m$ is the thickness of the clay layer.

The resulting match can be seen in Figure 5-6.

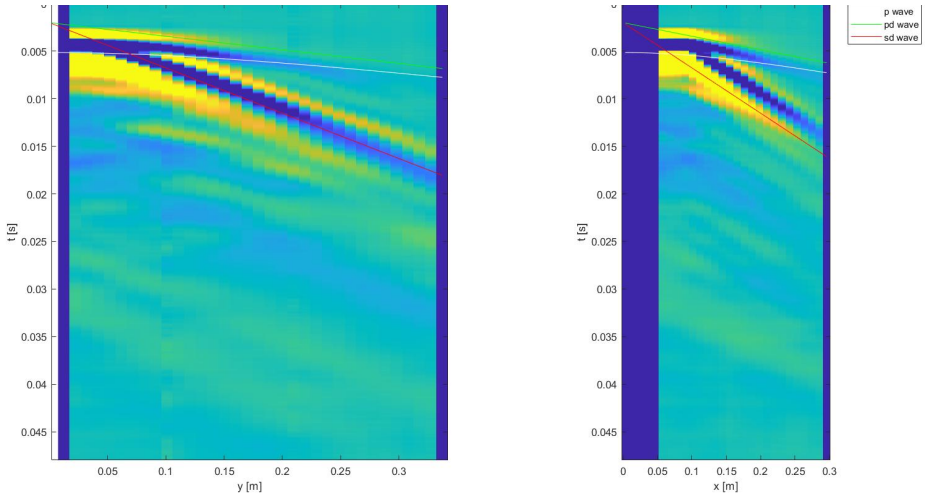

Figure 5-6: Analysis of tx and ty slices for the clay grid. In green and red, the direct P- and S-wave traveltimes are shown. In white, the reflected P-wave traveltime is shown.

Another event that stood out on the tx and ty slices is a hyperbola appearing as predominantly yellow amplitudes at $\sim 0.005\ s$. Initially, it was thought that this could be the reflection from the bottom of the box (i.e., from the interface between clay and the plastic crate). There was a second option, however, namely that it was from the floor of the laboratory. In fact, the analogue model is inside a wooden box but between the floor and the bottom of the clay there is a plastic crate that is mostly, but not completely hollow. However, if the wave indeed ran partially through the air and did reach the floor, then we should have seen two other layers with different associated velocities (RMS[3]): one with a much higher propagation velocity than the one we have here, close to the air wave velocity, and one related to the floor (hard rock). But this is not the case. Thus, the most reasonable interpretation is that reflection was from the bottom of the clay[4].

[3]The RMS velocity is possible to compute only for a model with many sublayers or at least two. We assumed the clay model is a single homogeneous layer model, but the reality is different.The clay layer was composed of four sublayers using 10 cm height clay bricks placed horizontally in the box (see section 4). However, the clay bricks are not equally distributed but some sublayers are thicker or slimmer than others. So we can think about the one layer model like internally divided in 4 sublayers of unknown thickness

[4]Furthermore, we can probably rule out this hypothesis because the transmission coefficients of elastic waves from solids into air are close to neglegible: usually, a free surface is considered to be a perfect reflector.

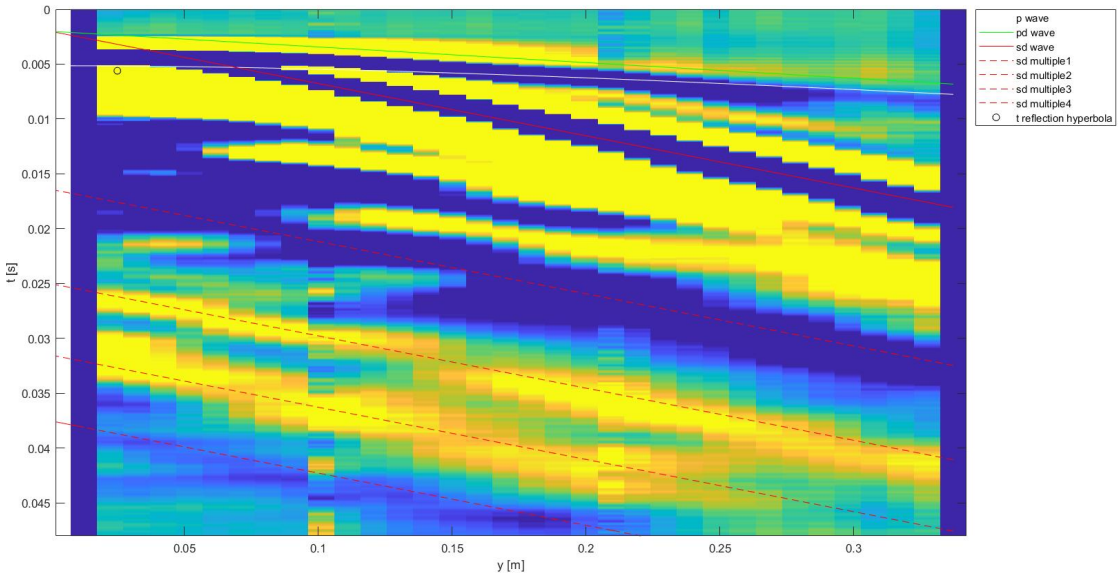

Figure 5-7: Analysis of SP Multiples of the Clay grid

Another possibility that was briefly considered was that the reflection could be from one of the sublayer interfaces. Indeed, the clay model was built with bricks of 10 cm thickness each which were placed in five sublayers, each compressed and compacted. Therefore, the exact heights of the sublayers are unknown: we just could measure the total height of the clay layer, which was around 45 cm. If we could see the reflections from the clay interfaces, however, then we should see five hyperbolas, not only one.

Note that the hyperbola is not the only additional event that stands out on the section. What stands out in Figure 5-6, for example, are some events that have the same slope as the direct S-wave but with different t_0. Such is the behaviour of multiples, for example. By using the same method as before, we can plot over the vertical section the theoretical multiples of the direct S-wave. The equations used were as follows:

$$t^S_{mult} = t^{mult}_0 + y/V_S \tag{5-7}$$

Where the multiples were four and the starting times of each were $t_{0,mult} = (0.0164, 0.025, 0.0315, 0.0375)s$. 5-7 shows a good match. As a consequence, I estimated the distance travelled by the equation:

$$h_{S,mult} = V_{S,mult} * t_{mult}/2 \tag{5-8}$$

The estimated heights are $h_{S,mult} = (0.1722, 0.2625, 0.3307, 0.3937)m$. They are 10 cm far from each other; thus it could be reasonable to state that these are not multiples but just the S direct waves for the clay interfaces of the last 4 layers. Therefore, the first direct S wave is the one that scattered on the first layer at $t0 = 0.002s$. In the end, the $h_{S,mult}$ is better to be name as h_S, a vector of 5 distances: $h_S = (0.02100, 0164, 0.025, 0.0315, 0.0375)m$. Because the surface on the source reference system is at 0.021 m, we can just subtract it to obtain the real heights of the sublayers.

$$z_{sublayer,clay} = h_S - h_{S,1} \tag{5-9}$$

$$Z_{sublayer,clay} = (0, 0.1512, 0.2415, 0.3097, 0.3727)m \tag{5-10}$$

$$H_{sublayer,clay} = (0.1512, 0.0903, 0.0682, 0.063)m \tag{5-11}$$

$$H_{clay,exp} = 0.3727m = 0.4m \tag{5-12}$$

Considering that they should be far 10 cm each, it makes sense.

Wavefront analysis for the one layer model

The second part of the processing consists of distinguishing the type of wave propagation visible in the time slices based on their wavefronts. Therefore, a change of coordinate system was done, from the coordinate system of the source, with the origin at its center, to the LDV coordinate system, which had the origin coinciding with one of the corners of the box. The main goal was to verify if the waves reflect from the wooden side walls of the box. Thus, I defined a mirror source, symmetrical to the real source with respect to the wall of the box along the y axis of the LDV reference system (see Figures 5-8a and 5-8b).

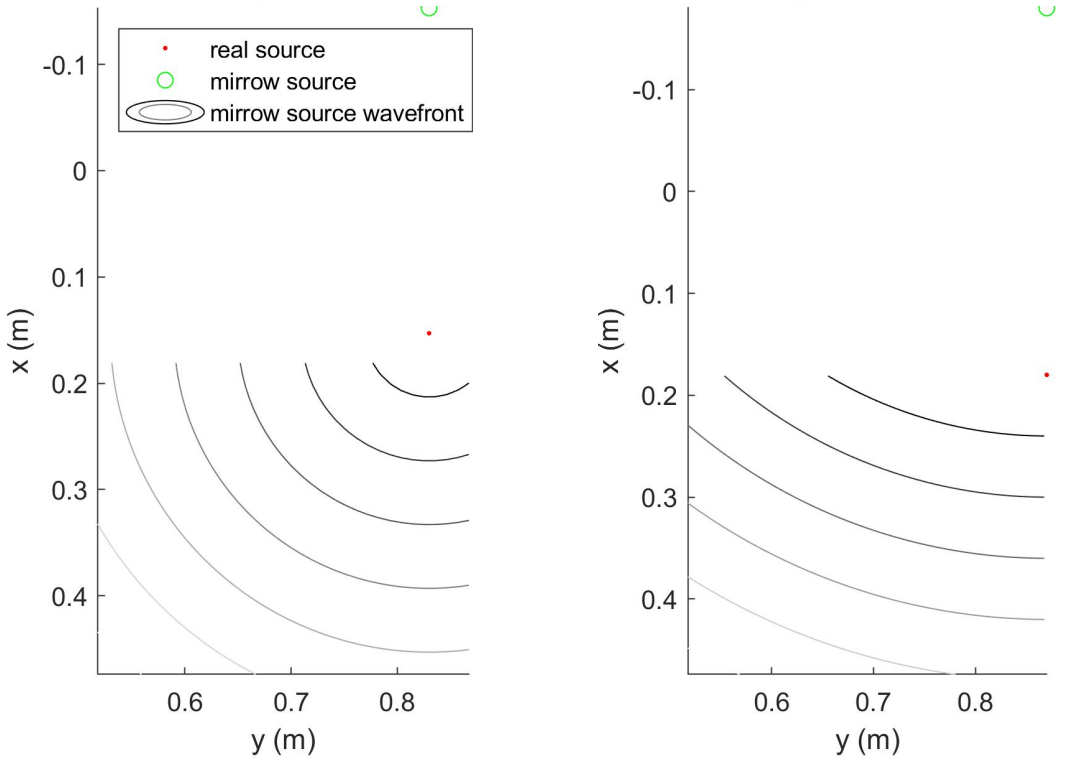

(a) Spherical wavefronts for the source.

(b) Spherical wavefronts for the mirror source.

Figure 5-8: Source wavefronts for the Clay grid.

The equations for the wavefronts (i.e., surfaces of constant propagation time) of the real and mirror source are as follows:

$$t_{src}^{real} = \sqrt{(x - x_{src}^{real})^2 + (y - y_{src}^{real})^2}/V_P \tag{5-13}$$

$$t_{src}^{mirror} = \sqrt{(x - x_{src}^{mirror})^2 + (y - y_{src}^{mirror})^2}/V_P \tag{5-14}$$

where $(x_{src}^{real},\ y_{src}^{real}) = (0.17,\ 0.84)\ m$ are the coordinates of the real source and $(x_{src}^{mirror},\ y_{src}^{mirror}) = (-0.17,\ 0.84)\ m$ the coordinates of the mirrored source.

Equations 5-13 and 5-14 were then used to compute traveltimes for all the xy locations of the recording grid and the traveltimes contoured using the matlab function *contourf*. The resulting contours for the direct and mirror source can be seen in Figures 5-8a and 5-8b, respectively. These contours were subsequently overlapped on several time slices of the velocity for a time window in which several events were observed. It turns out that the waves could be distinguished straightforwardly between direct waves and waves from the mirror source (i.e., reflected waves).

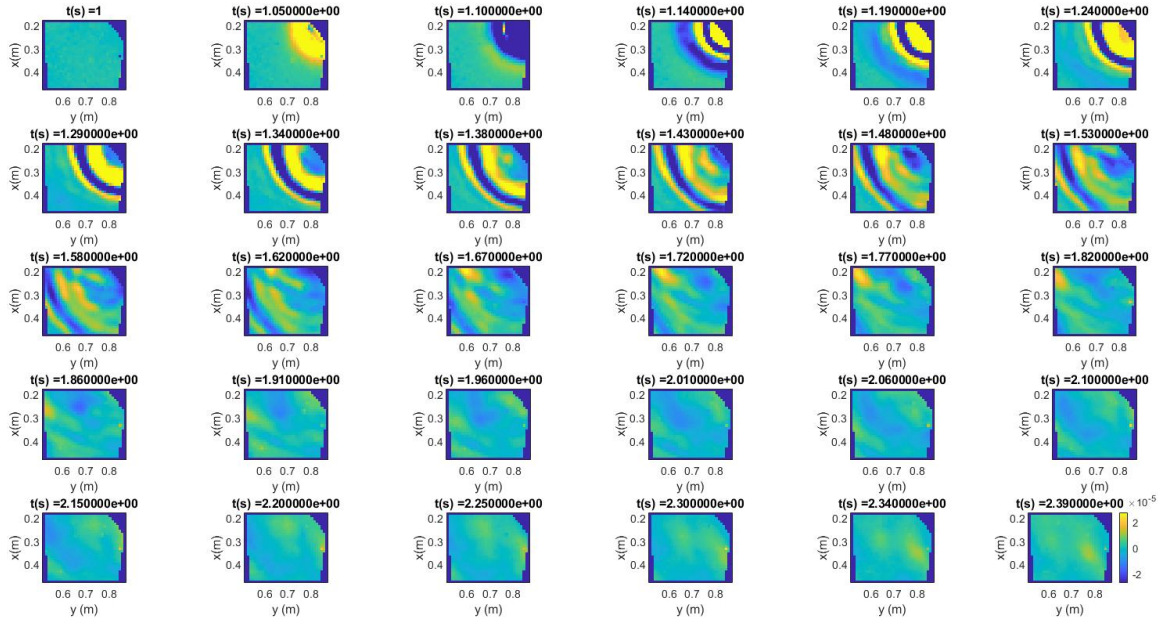

Figure 5-9: Time slices of the clay grid. The Figure shows the waves as a response of the clay to the source input during time

Looking at Figures 5-11, 5-12, and 5-13, we can confidently say the wall of the box does have an influence on the scattering of the waves.

Conclusions for the processing of the one layer model

The two processing analyses brought two types of results, one quantitative; the magnitude of the wave velocities, and one qualitative; the identification of the nature of the propagated waves. For the first point, in summary, the events seen are:

$$\text{Direct P-wave with } V_p = 70\ m/s \tag{5-15}$$

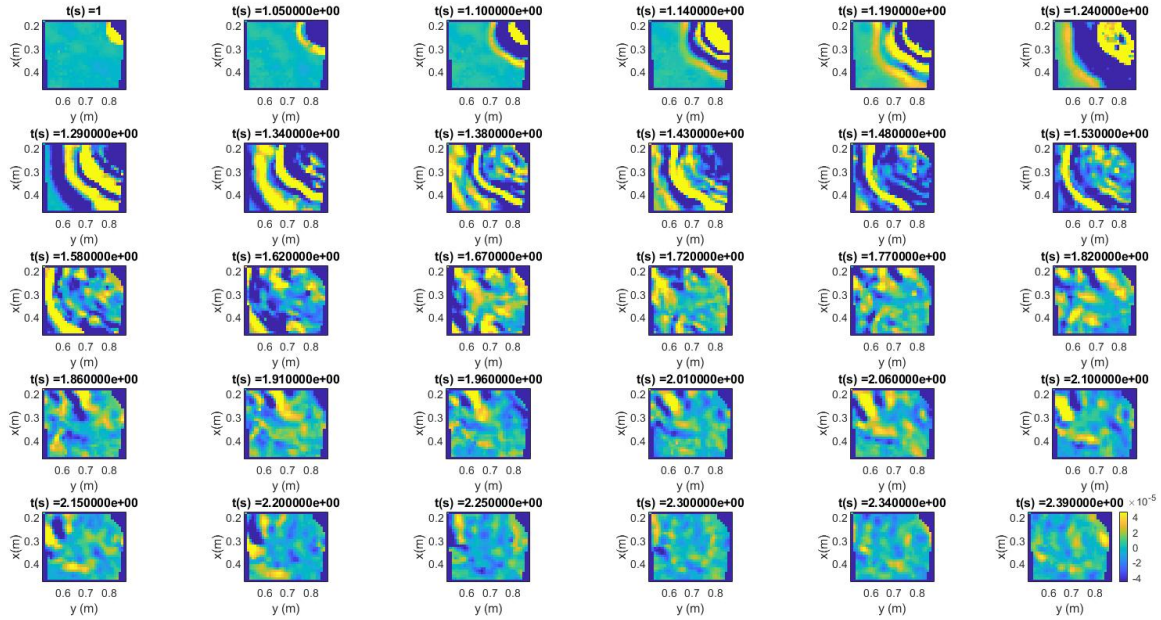

Figure 5-10: Time slices of the sand grid. The Figure shows the waves as a response of the sand to the source input during time

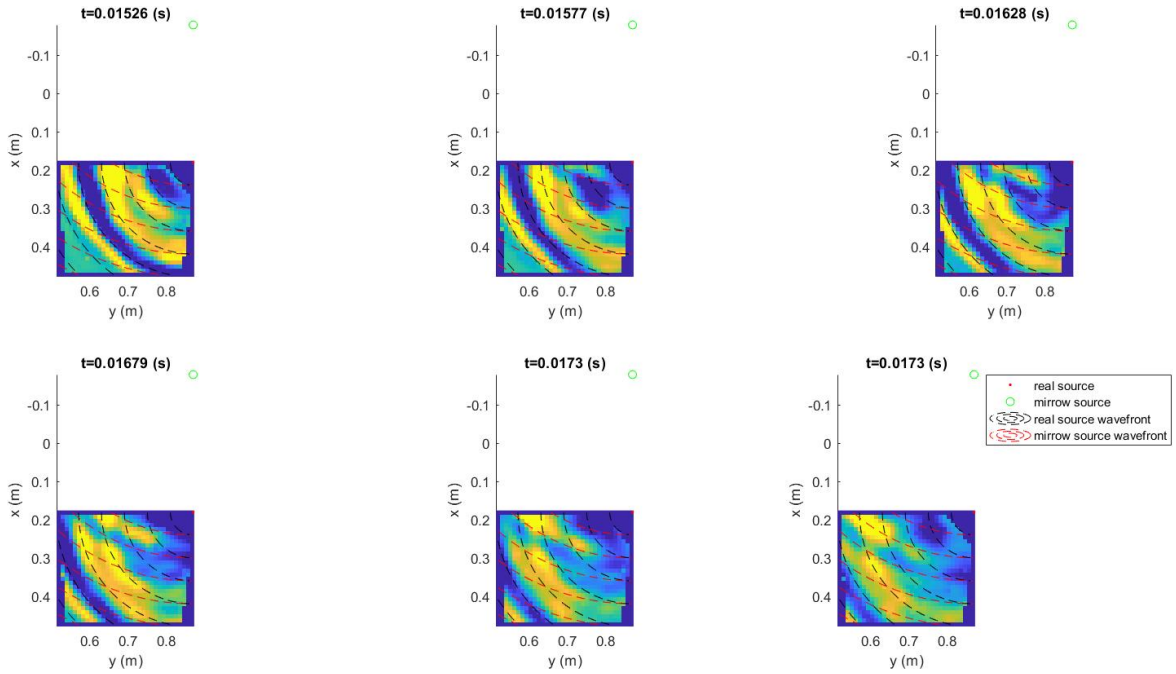

Figure 5-11: Analysis of direct and reflected wavefronts for the Sand grid (Later times).

$$\text{Direct S-wave with } V_s = 21\ m/s \tag{5-16}$$

$$\text{S waves at } t = (0.0164,\ 0.025,\ 0.0315,\ 0.0375)\ s \tag{5-17}$$

$$\text{Reflected P-wave from the bottom of the clay with } V_{RMS} = 80\ m/s \tag{5-18}$$

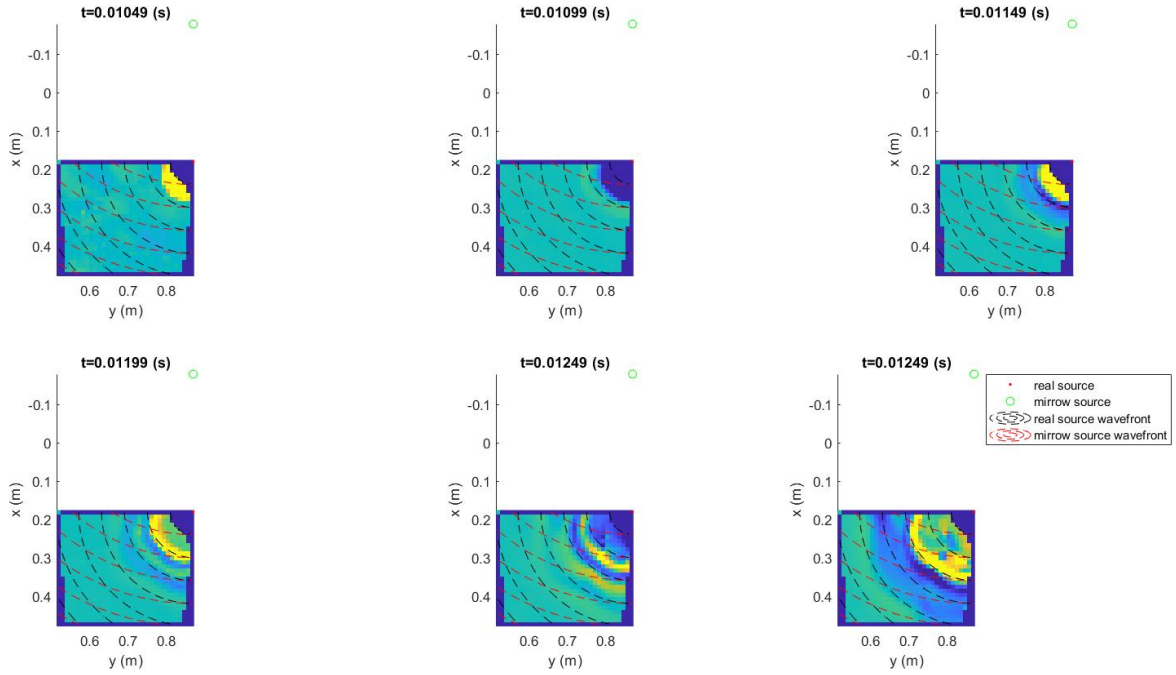

Figure 5-12: Analysis of direct and reflected wavefronts for the Sand grid (Earlier times).

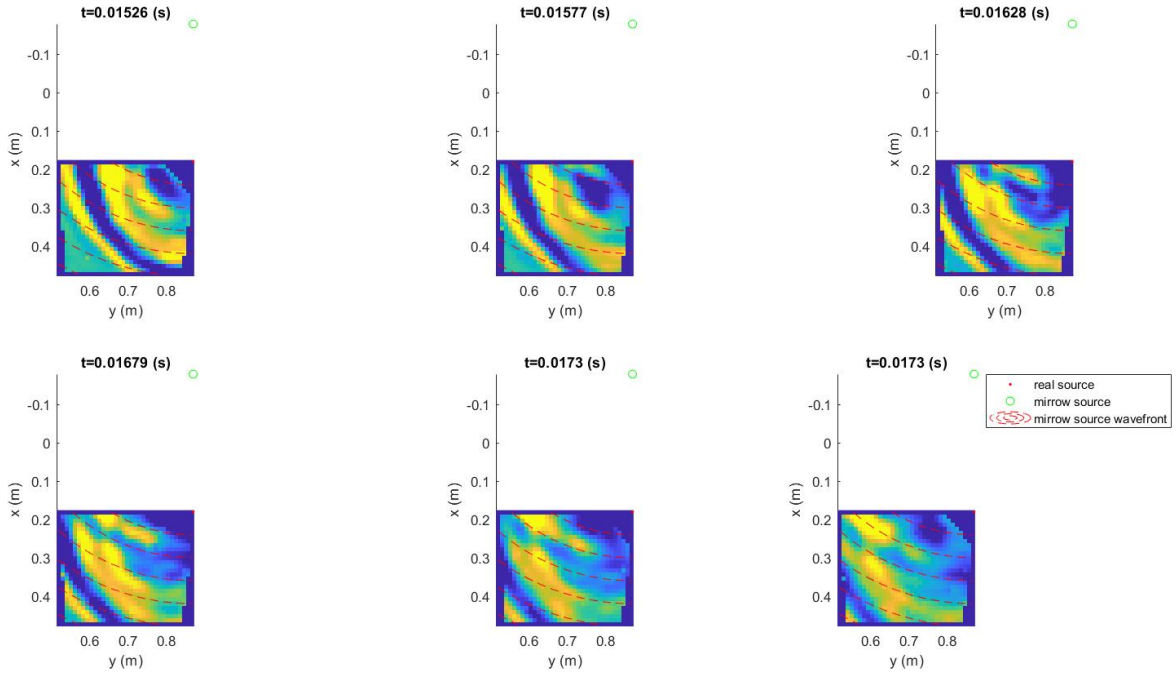

Figure 5-13: Analysis of direct and reflected wavefronts for the Clay grid

$$\text{Thickness of the sublayers, } z_{sublayers} = (0.1512,\ 0.2415,\ 0.3097,\ 0.3727)\ m \tag{5-19}$$

While for the qualitative analysis, the wavefronts originate from the real source and the mirror

source[5]. No other reflections appeared in time slices studied: for example we do not observe for the clay any dots on the time slices similar to what we see for the case of the sand (see Figure 5-5). Moreover, reflections from the interfaces of the clay sublayers may be visible and most likely they are S waves. Provided that this interpretation is correct, we are confident to relate the value of h_{clay} to the V_{RMS} of the hyperbolic event at t_{hyp} and state that the strong reflection at 0.005 s is the P-wave reflection from the bottom of the clay.

Results for the two layer model

Experiment 2 was processed in the same way as Experiment 1, as described in section 5-2-1. As can be seen in the flowcharts in Figures 5-1 and 5-2, the velocities of the clay were used as an input for the Wavefront Analysis of the sand. In fact, the two layer model maintains the clay characteristics and knowing how the clay behaves in the box was crucial to distinguish the sand responses. The P- and S-waves of the clay were plotted on top of the tx and ty slices together with the characteristic waves of the two layer model. Comparing Figure 5-6 to Figure 5-15 should make this point clearer. A comprehensive understanding of the two layer model stressed by an impulsive source was reached thanks to the additional information obtained from the experiment on the clay.

However, going through the processing step by step, the sand surface was much more regular than the clay; because of the material's nature, it was much easier to handle. The slices of constant t, x, and y at the same positions as the clay are shown in Figure 5-5. Here, the values of the velocities of the direct waves of the sand are:

$$\text{Direct P-wave with } V_p = 50\ m/s, \text{ and} \tag{5-20}$$

$$\text{Direct S-wave with } V_s = 30\ m/s. \tag{5-21}$$

They are highlighted in Figure 5-17 and Figure5-15.

Returning to Figure 5-5, there are the two spots we called P_1 and P_2 (paragraph 5-2-1). To study them, I plotted two lines that mark their position on the tx and ty slices, see Figure 5-14. In the area immediately below the direct wave there is an unclear interference pattern, like a ringing. The red and black lines go through exactly that interference pattern. This observation prompted me to consider that the spots and the interference are related. In fact, imagine we are sitting on the sand surface, looking at the waves from the top, i.e., the xy plane, then what we see of a reflected spherical wave propagating upwards is just its head: a horizontal section of a hyperboloid. From our point of view, it would just be a circle but initially it would be a dot. In reality, the wave goes through many distortions so instead of a circle, it looks like a deformed spot. Exactly like our P_1 and P_2. Furthermore, the direct wave from the source means that we see the superposition of that event and the reflected wave. Keeping in mind this idea, that P_1 and P_2 may be the reflection from the Sand-Clay interface, how can we justify it? With the velocity analysis, like we did for the clay. Again we compute the velocity for the hyperbolic event using its zero-offset two-way traveltime picked on Figure 5-15:

$$t^P_{reflected} = 0.012\ s \tag{5-22}$$

[5]We thus note that only the closer side wall of the box aligned with the y axis seemed to produce reflections. The farther side wall aligned with the x axis did not seem to produce any.

As we have seen previously, the equation for a reflected wave is:

$$t^P_{reflected} = t_0 + \sqrt{(2d)^2 + y^2}/V_P. \tag{5-23}$$

Evaluating at zero-offset we obtain:

$$t^P_{reflected}(y = 0) = t_0 + 2d/V_P. \tag{5-24}$$

This yields the following expression for d:

$$d = V_P \cdot (t^P_{reflected} - t_0)/2. \tag{5-25}$$

Plugging in the values we find: 0.11 m [6]. And that is exactly the height of the sand layer expected[7]. Furthermore, if we add H_{sand} to the H_{clay} we go back to the total height of the two layers model, that is $H_{model} = 0.49\ m$. Close to the one measured with a tape measure in the laboratory (around 45 cm). We can say we are happy with this result and it can be considered as a confirmation of our interpretation. Note that in Figure 5-14 the horizontal white line intends to highlight the time of the reflection. There is a blue coloured reflection that is related to the Sand-Clay interface.

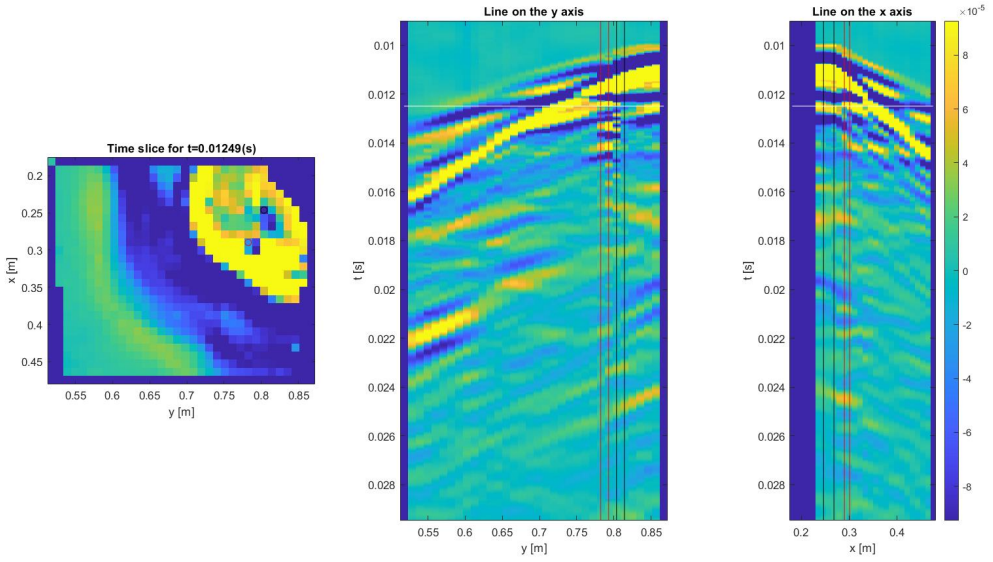

Figure 5-14: Analysis of the reflection from the interface Sand

A few events are not completely understood. In Figure 5-15 between the direct S wave and the next S wave there are three groups of amplitudes. For clarity, I highlighted them with three ellipses in Figure 5-16. The black and red ellipses have a change in phase(e.g., there is blue-yellow-blue amplitudes in the black ellipse while there is yellow-blue-yellow amplitudes in the red ellipse). While the event in the grey circle appears a hyperbolic reflection. The

[6] It would be interesting for future works to dedicate some extra time to the structure of the Clay and the Sand-Clay model in order to have a clear idea of its interference with the soil signal. In this thesis we did not go into too much details, because the main goal is to study the non linearity in the sand layer

[7] The desired thickness of the sand layer was 12 cm

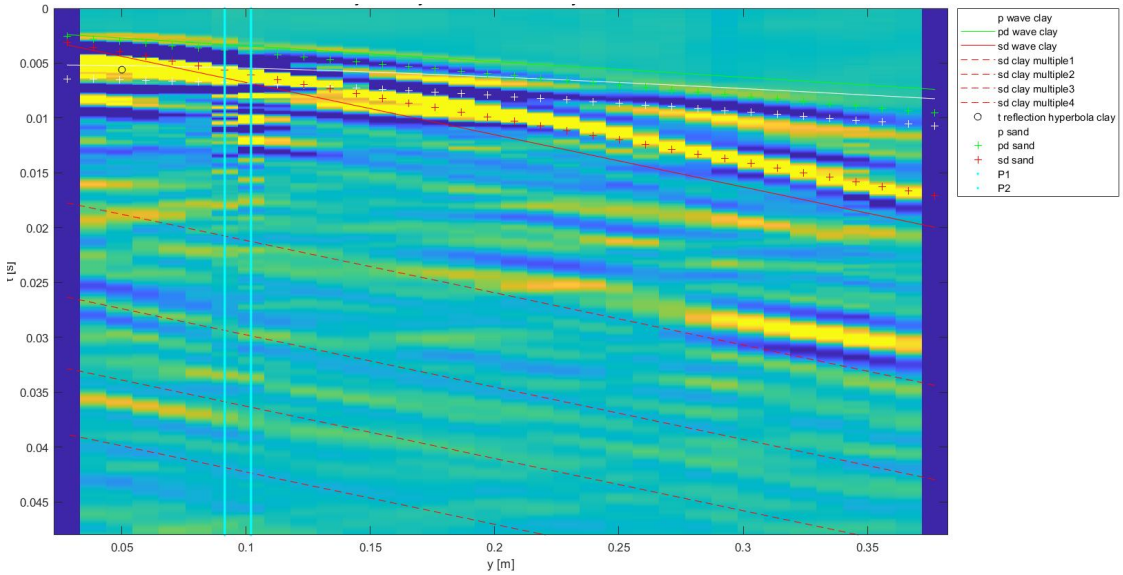

Figure 5-15: Analysis of Clay events on the Sand-Clay vertical section

reflection seems to experience an interference with another event that deforms its typical shape. It seems possible that the event interfering could be the one in the black ellipse. A hypothesis would be that they are conform to the mirror source, so correspond to scattering form the walls. Anyway, their nature is still unclear.

Wavefront analysis for the two layer model

Next, we discuss the wavefront analysis for the two layer model. This appears much more interesting than the clay, due to its variety of events. We used the same method described in section 5-2-1, but with a larger time window. Results can be seen in Figures 5-18 to 5-21, while for extra details you can refer to Figures 5-13, 5-8a, and 5-8b.

Conclusions for the processing of the two layer model

In conclusion, direct P- and S-waves, S-wave multiples and the reflection from the bottom of the clay found in the one layer model are still visible in the recorded data for the two layer model. Plotting the clay characteristic waves on the ty slice for the two layer model helped to isolate the sand characteristic waves. They are: direct P, direct S of respectively 50 m/s and 21 m/s and the reflections from the sand-clay interface. Furthermore, some extra events were identified but their nature is still not fully understood. A hypothesis would be that they correspond to scattering from the walls of the wooden box.

Interpretation

Regarding the one layer model, the events seen are:

- Direct P-wave with $v_p = 70\ m/s$

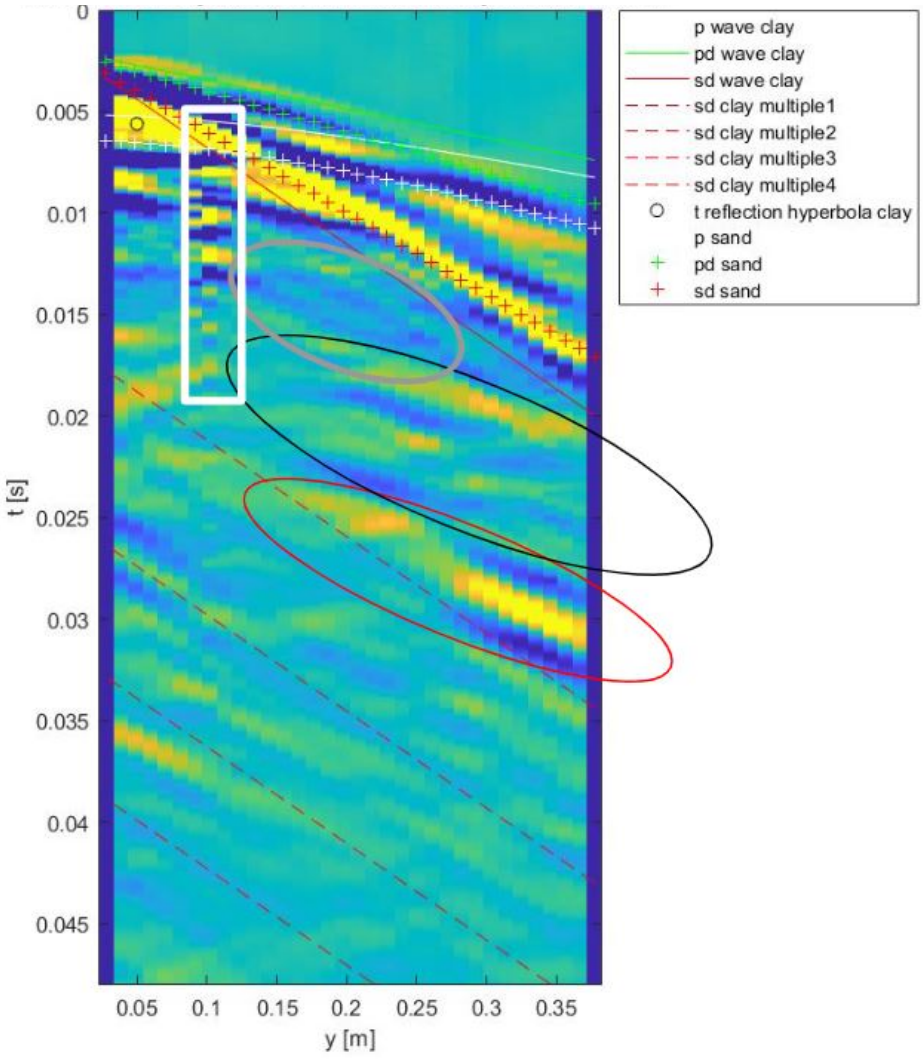

Figure 5-16: Analysis of Clay events on the Sand-clay vertical section with highlights. The white rectangle shows the deformations of the amplitudes due to the reflection from the sand-clay interface. While the colored ellipses highlight events, of which we did not understand the nature

- Direct S-wave with $v_s = 21\ m/s$
- S-wave multiples at $t = (0.0164, 0.025, 0.0315, 0.0375)\ s$
- (hyperbolic event) Reflection from the bottom of the clay
- Wall reflections consistent with a mirror source

No other reflections appear in time slices studied.

Regarding the two layers model, the events seen are:

- The Clay characteristic waves (as above).

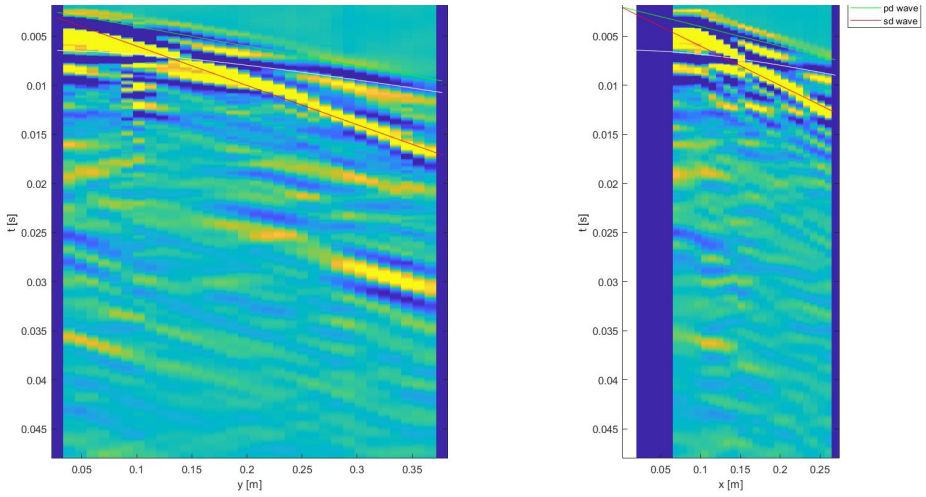

Figure 5-17: Analysis of tx and ty slices for the sand grid. In green and red, the direct P- and S-wave traveltimes are shown. In white, the reflected P-wave traveltime is shown.

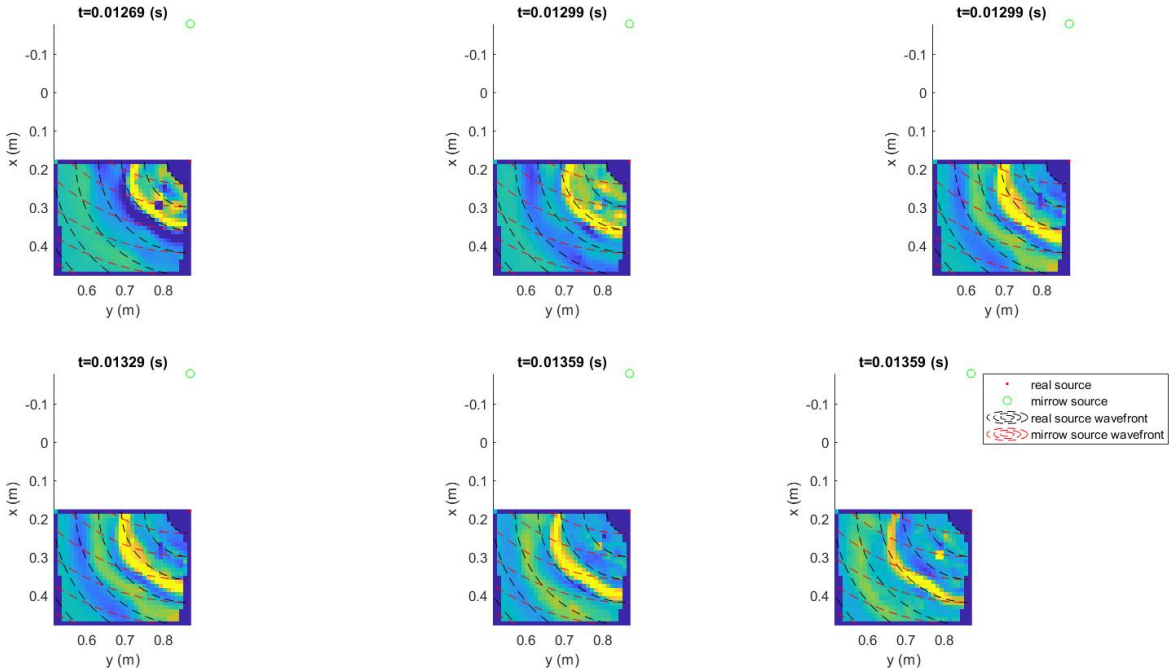

Figure 5-18: first part of the analysis of the wavefronts of the Clay grid

- The Sand characteristic waves:
- Direct P-wave with $v_p = 50\ m/s$
- Direct S-wave with $v_s = 30\ m/s$
- Reflection from the bottom of the clay

Some extra events were identified but not still understood.

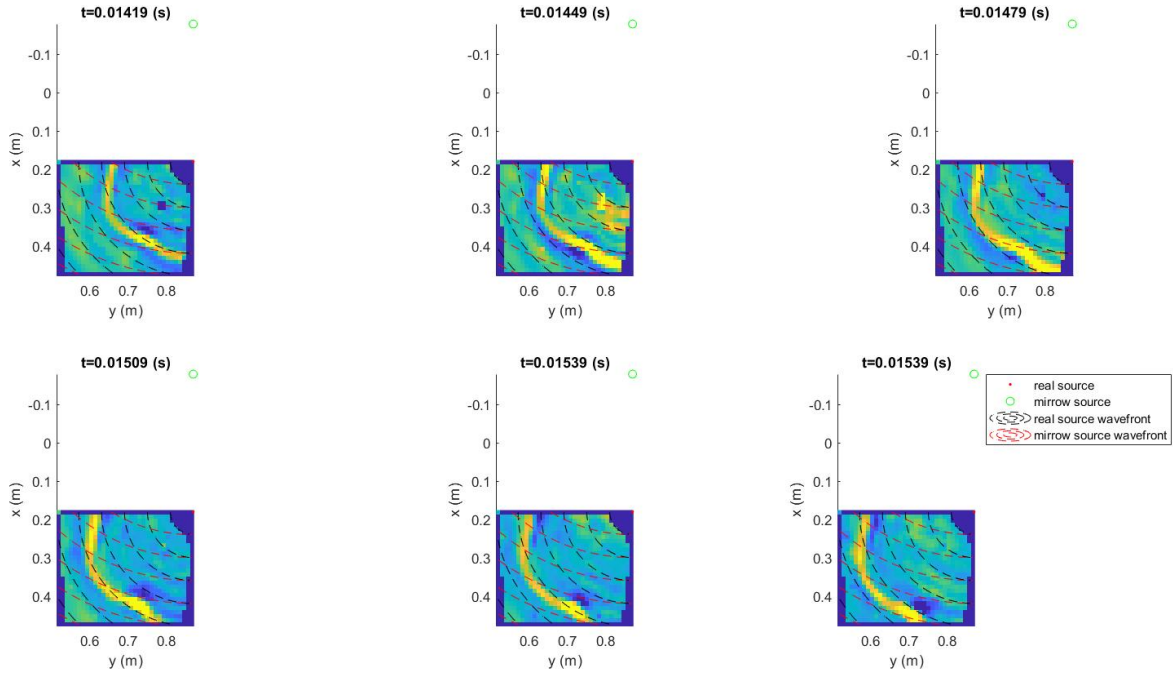

Figure 5-19: Second part of the analysis of the wavefronts of the Clay grid

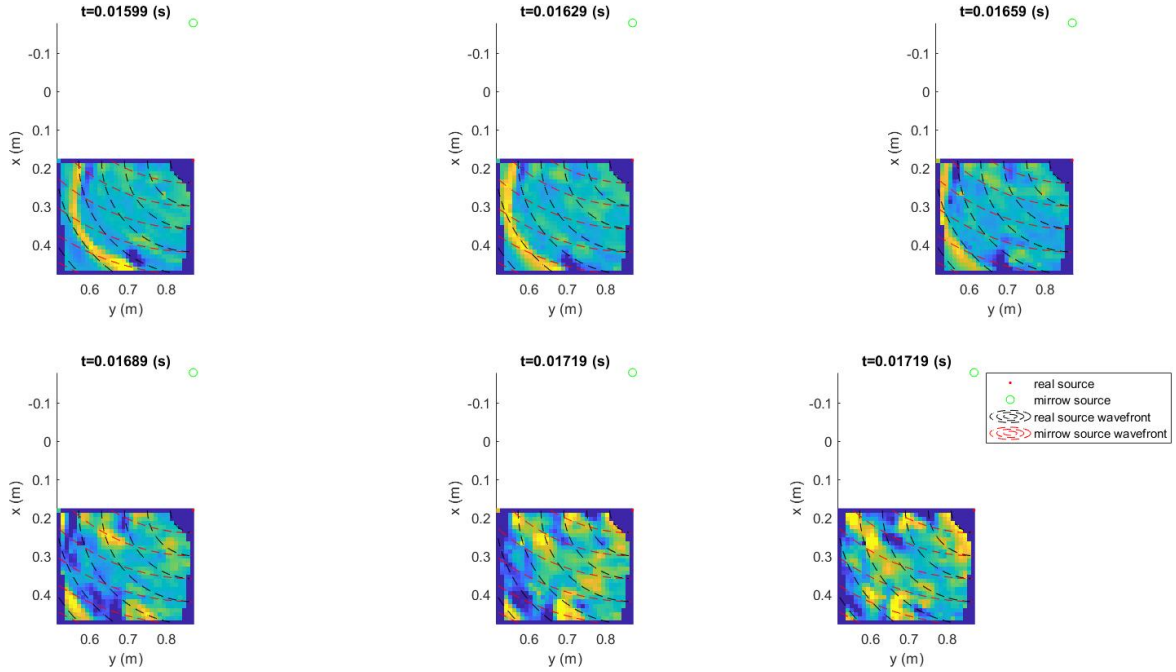

Figure 5-20: Third part of the analysis of the wavefronts of the Clay grid

This concludes the interpretation of all the phenomena we noticed related to the box structure and the one and two layer model. Now, we have enough information to study the non-linearity, first of the one-layer clay model and then of the two layer sand-clay model. Subsequent experiments will be carried out with a sweeping sinusoidal source for a diagonal line across

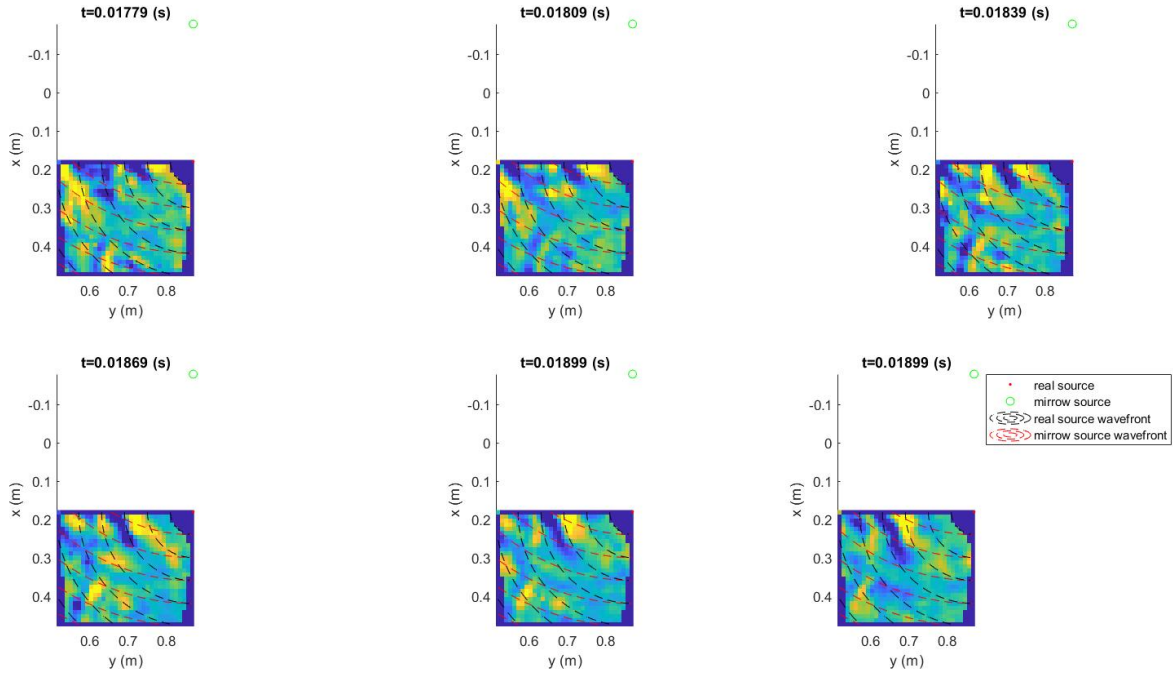

Figure 5-21: Fourth part of the analysis of the wavefronts of the Clay grid

the grid originating from the piezoelectric source.

5-2-2 EXPERIMENTS 3 & 4: NON LINEARITY OF THE 1 & 2 LAYER MODEL

Setup

The setup used was the same as for experiments 1 and 2. The difference is in the source signal and in the receiver positions acquired. In fact, this time the base signal was a sinusoid, and the input was a sweep over a broad range of frequencies. The parameters can be found in Table 5-1.

5-2-3 Acquisition

We based our setup and acquisition method to the papers of Boaga [2021], Lawrence and Brackman [2008] and Johnson [2009]. The source sweeps over a frequency bandwidth of one octave. We acquired 16 times the response on a diagonal line of the grid for the one and two layer model; one for each different value of the Voltage level. Those levels are from 50 mV to 800 mV with steps of 50 mV, before amplification by the amplifier by a factor of 100. The aim is to excite a non-linear behaviour of the sand using such a strong source sweep. We would like to recreate on a smaller scale the large ground motions above 1g already reached by previous field work experiments on a 1:1 scale [Lawrence and Brackman, 2008]. Thus, Experiment 3's main aim is to characterise the response of the clay under such source sweep signals.

	generator		LDV
Amplitude High	50-800 mV_{pp} with step of 50 mV	n points	845
Voffset Low	250 mVdc	n stack	200
Width Duty	400 mus	sampl. f	100 kHz
Edge Time	100	samples	4800
Frequency period	100000	delay in t	50 ms
		trigger input	internal
	source		
signal	sin		
type of input	sweep		
n cycles	1		
trigger	external		
direction trigger	raising		

Table 5-1: Acquisition setup used in the non-linearity experiments

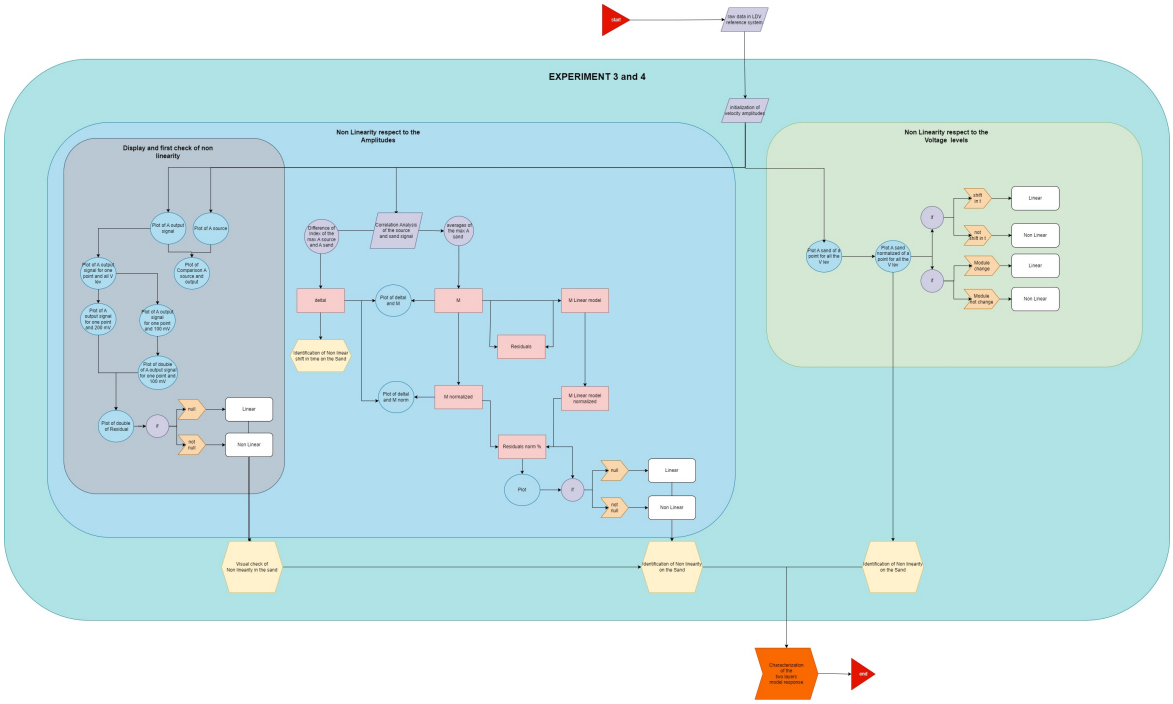

Figure 5-22: Flowchart for Experiments 3 and 4

5-2-4 Data Processing

Non-linearity with respect to the Amplitudes

As for Experiments 1 and 2, I wrote two codes; one for each of the models, with the same processing analysis, displayed in Figure 5-22.

Overall, the analysis of the non-linearity is divided in two sub analyses: one focusing on the non-linear amplitude behaviour and the other on the non-linear time-delay behaviour of the output signal (both as a function of the voltage input level). For simplicity, we will call them:

Non linearity with respect to the Amplitude and Non linearity with respect to the Voltage level (see Figure 5-22). Starting with the former, the first step is visualising the signals doing a first check of non-linearity. Figures 5-23a and 5-23b help to get an idea of the type of signals that we are dealing with (for extra figures see 5-24a, 5-25a, 5-24b, and 5-25b).

The analogue model materials (i.e., the clay and the sand) absorb the majority of the swept source signal: the amplitudes are considerably smaller compared to the impulsive experiment. The amplitudes decrease in value with the distance to the source, as expected (Figures 5-26a and 5-26b), while the variation in amplitudes with respect to the voltage levels is evident in Figures 5-27a and 5-27b.

We know that in a linear scenario, if the input voltage doubles, also the amplitude of the output signal should double. Therefore, I displayed the amplitude for a central recording point in the diagonal line for voltage level 4 and double the amplitude for voltage level 2, to do a first raw analysis. They overlap but with some discrepancies, see Figures 5-28a and 5-28b. Considering the residuals in Figures 5-29a and 5-29b, we see that the residual for the two layer model is considerably bigger than for the one layer model.

If the signal was linear then the residual should be very small or null. If it is not, it means it is not. Of course, this is just a first, raw, qualitative look at the output signals that cannot give any reliable results, but looking carefully at the displays of the signals is fundamental to start the processing analysis. Besides, three important questions arose from the comparison of the model and the source signals:

- How can we separate the difference between the source and the soil response?
- How can we quantify the relationship between the amplitudes and the voltage level?
- How can we estimate if the varying voltage levels cause time-lags in the soil signal?

Consequently, two new matrices were defined to try and answer those questions: ΔI and M.

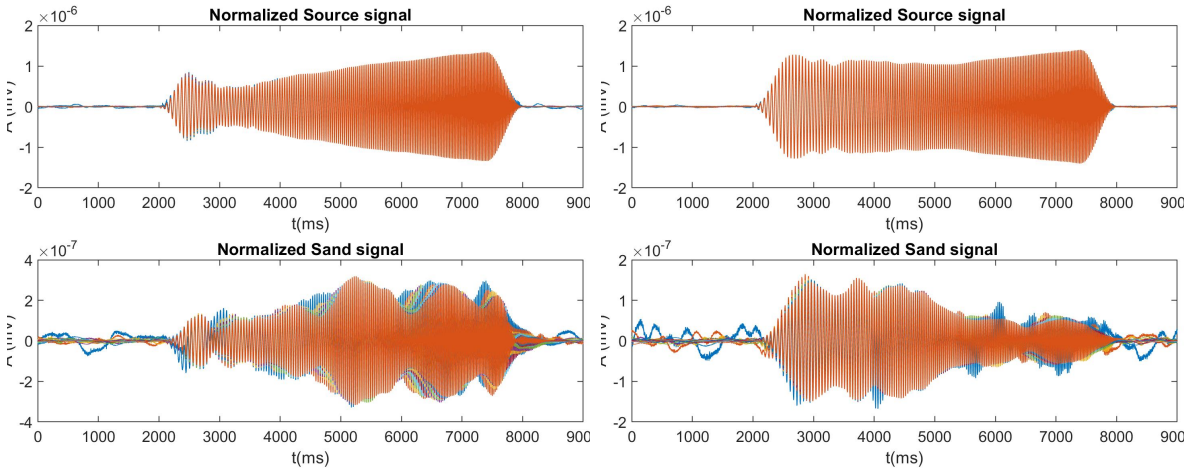

Figure 5-23: Normalized source and soil signals for (a) Two layer model and (b) One layer model.

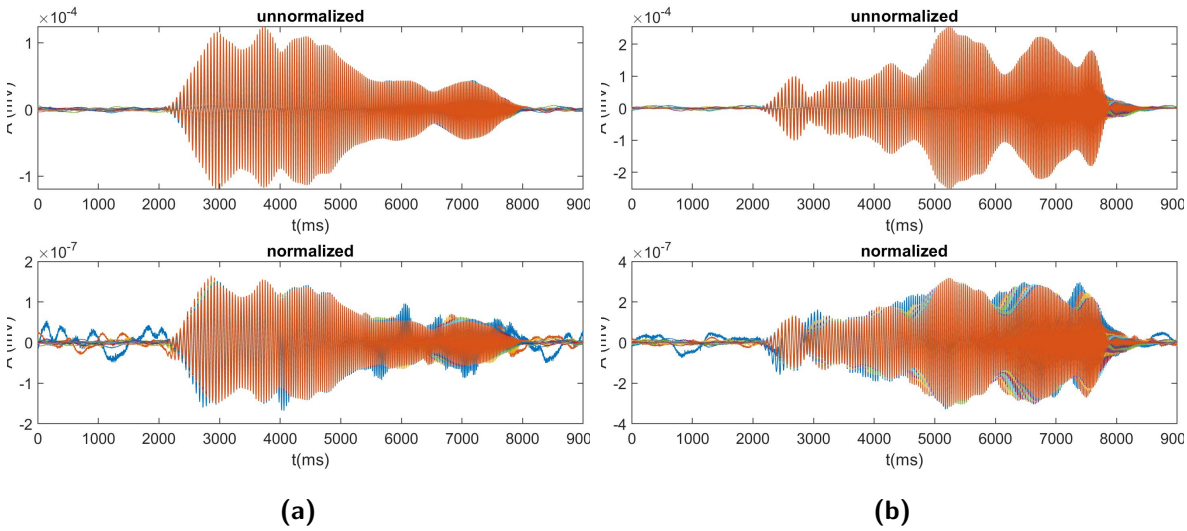

Figure 5-24: Raw and normalized soil signals for (a) Clay model and (b) Sand-Clay model.

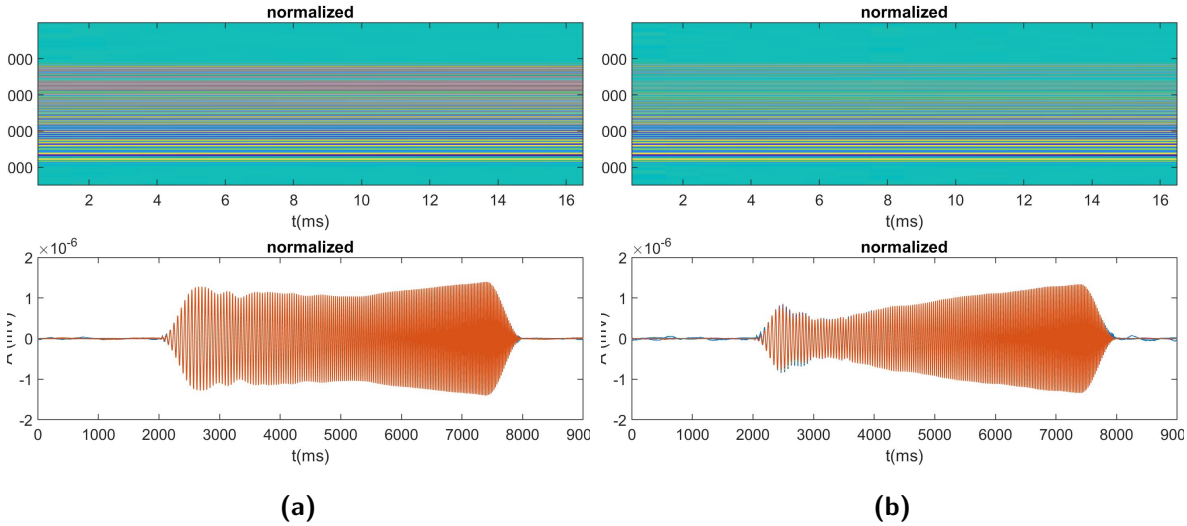

Figure 5-25: Normalized source signals as images and waveforms for (a) Clay and (b) Sand-Clay.

To separate potential time-lags due to varying voltage from normal, propagation-related changes in phase along the line of recordings, we first cross-correlated the soil signal with the source signal for a particular, fixed analysis location (i.e., fixed i) and for the highest voltage (i.e., maximum j) to estimate the propagation-related delay by finding the index of the cross-correlation maximum. We then shifted all the soil signals for the varying voltages by the same time delay, essentially removing the normal, propagation-related phase for that particular analysis point.

Then, we computed the maxima of the source signal and the shifted soil signal, and the indices at which these maxima occurred, in a chosen time window[8] for all voltage levels and we defined ΔI as the absolute value of the difference in index of the source and soil maximum,

[8]For the clay, the time window was 0.3099 s to 0.3139 s. For the two layer model it was 0.3049 s to 0.3099 s.

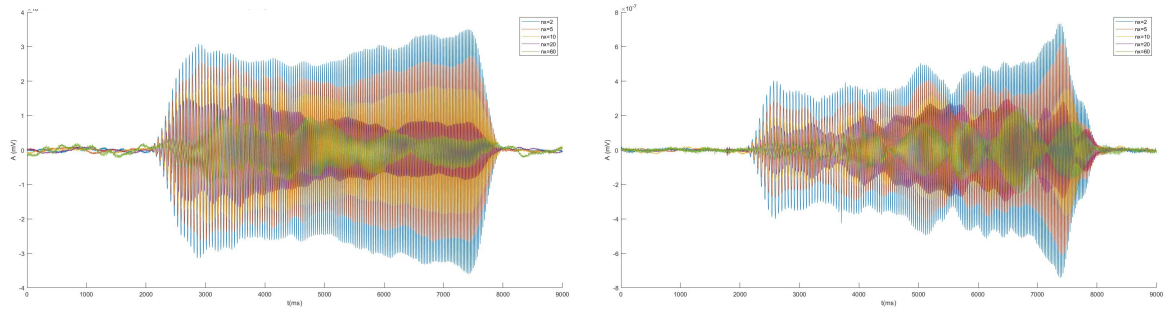

(a) **(b)**

Figure 5-26: Soils signals along the line for fixed voltage for (a) Clay and (b) Sand-Clay.

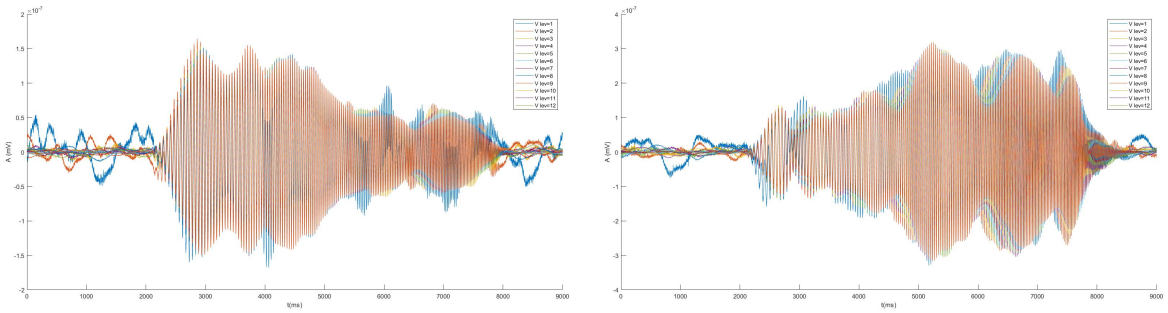

(a) **(b)**

Figure 5-27: Soils signals for all voltage levels for (a) Clay and (b) Sand-Clay.

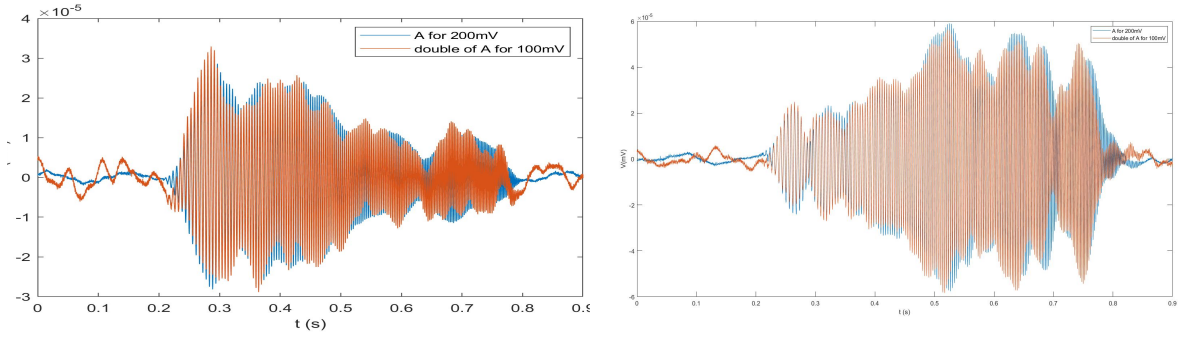

(a) **(b)**

Figure 5-28: Linearity check of the amplitudes for (a) Clay and (b) Sand-Clay.

while M is just the matrix of the maximum amplitude values of the soil. In equations:

$$\Delta I(i,j) = |Index_{source\ signal(i,j)} - Index_{soil\ signal(i,j)}| \tag{5-26}$$

$$M(i,j) = max[soil\ signal(i,j)] \tag{5-27}$$

where i denotes the point of the line, and j denotes the voltage level.

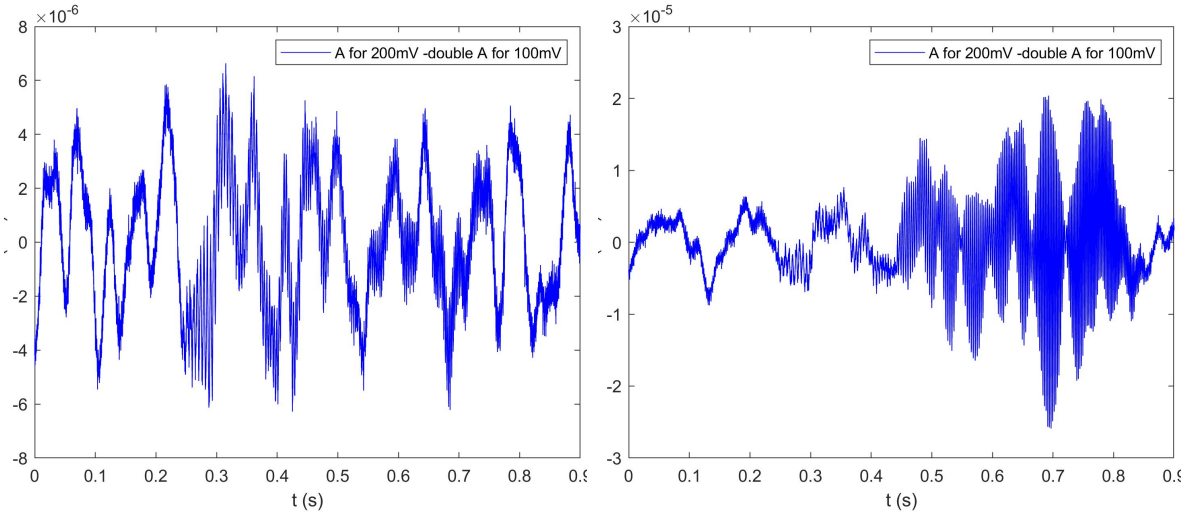

Figure 5-29: Analysis of the residuals for (a) Clay and (b) Sand-Clay.

However, this description of the computation of the matrix M is not complete. Note that at the beginning of the processing we already normalized the velocity amplitudes to the voltage level of the source. Now, we computed M from those normalised signals, thus we are working with already altered input. As a consequence, M can not be directly used for the subsequent analysis of the behaviour of the amplitudes respect to the voltage.

More specifically, it is not possible to analyse the behaviour of the soil using a generic expression such as equation 5-31, because the exponential factor would be any longer valid. In fact, if you use M without further changes, you will see that the amplitudes decrease their magnitudes with the distance from the source and there is no exponential relationship between the maximum amplitudes with respect to the V levels. Regarding the first point, we can remove the dependence to the distance by normalizing with the maximum amplitude for the highest voltage for each point along the line. We name the the matrix M that was normalized for the distance from the source $M_{distnorm}$. While the second issue is solvable by re-multiplying for the voltage level. In equations:

$$M_{distnorm} = M./M(:, 16) \tag{5-28}$$

$$M_{notnorm} = M_{distnorm}. * Voltages \tag{5-29}$$

$$M_{observed} = M_{notnorm} \tag{5-30}$$

where $Voltages$ is a row vector specifying all the voltage levels and equations 5-28 and 5-29 employ Matlab's implicit expansion notation. The resulting and M matrices for the one and two layer models are shown in Figures 5-30 and 5-31, respectively.

Nevertheless, the matrix M still does not give any quantitative information at this point. So, what we did was comparing it to a model that behaves linearly with respect to the voltage levels. We called the new matrix M_{model}. The idea is to look at the residuals between M and M_{model}. This model was built considering the "iterative" behaviour of the voltages. More specifically, we take advantage of the fact that the even voltage levels 2, 4, ..., 16 are doubles

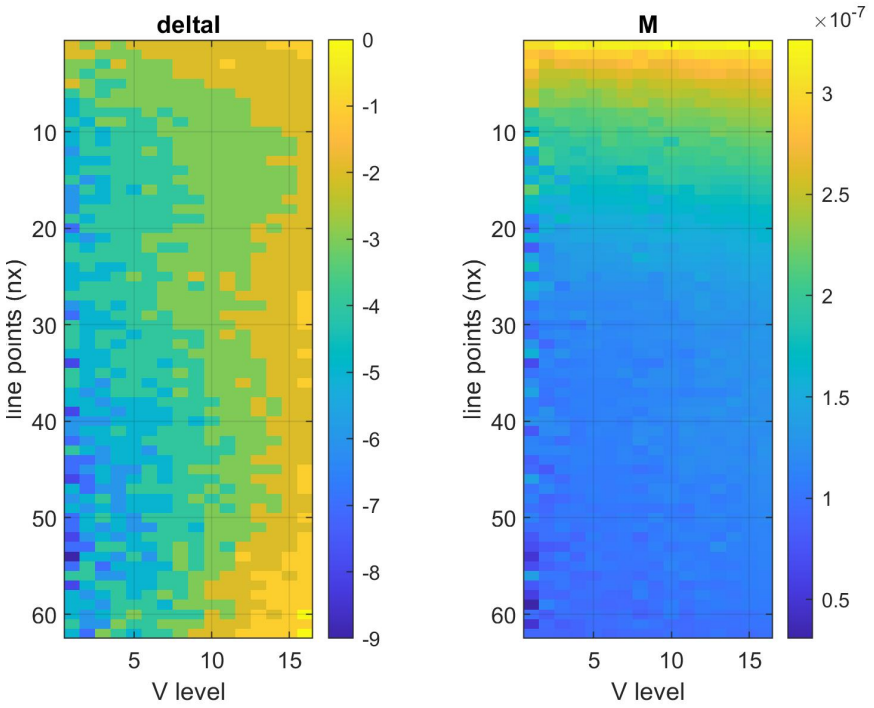

Figure 5-30: ΔI and M matrices for the one layer model

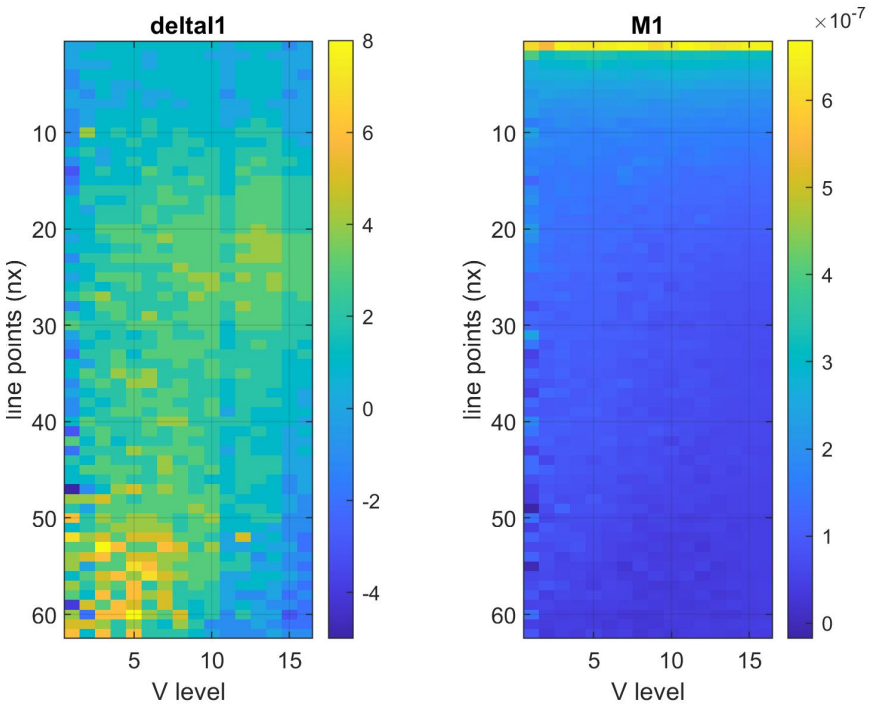

Figure 5-31: ΔI and M matrices for the two layer model

of the other voltage levels. We knew that theoretically a linear body should answer to the double the voltage with double the amplitude. In case, the body does not behave linearly, the coefficient with which the amplitude is multiplied is not two. In equations, if $f(x)$ is a general function we want to study and x is the voltage level in our case, then:

$$f(2x) = Cf(x), \quad \text{and} \tag{5-31}$$

$$C = 2^p, \tag{5-32}$$

where C is called the linearity coefficient and p is a constant parameter. If $C = 2$ (or $p = 1$) then the function is linear, if not then it is not linear. $M_{observed}$ is used to build the model, because it is free from any dependency to space and inputs. The model is dependent on an exponential parameter p. More than the model itself, what provides readable information is the residual between the model and the observed data. The residual indicates how far they are from each other, so our goal is to minimize the residual, because that identify the best fit value of the p parameter. Formalizing this gives:

$$Model(:,\ 2{:}2{:}16) = (2^p)M_{observed}(:,\ 1{:}8) \tag{5-33}$$

$$Residual = M_{observed} - Model \tag{5-34}$$

where for simplicity, we have again employed Matlab indexing notation. Note that the values for the Voltage levels 1:2:15 are not derivable, so those columns of the matrix are the same as in the observed data. The residual for those columns will be null by definition. To make the residual matrices more visually pleasant, we can just focus on the not null columns of the residual. Figures 5-32 and 5-33 display the matrices involved. (The colour bar goes from dark blue to yellow for increasing amplitude values). By comparing the residual of models for

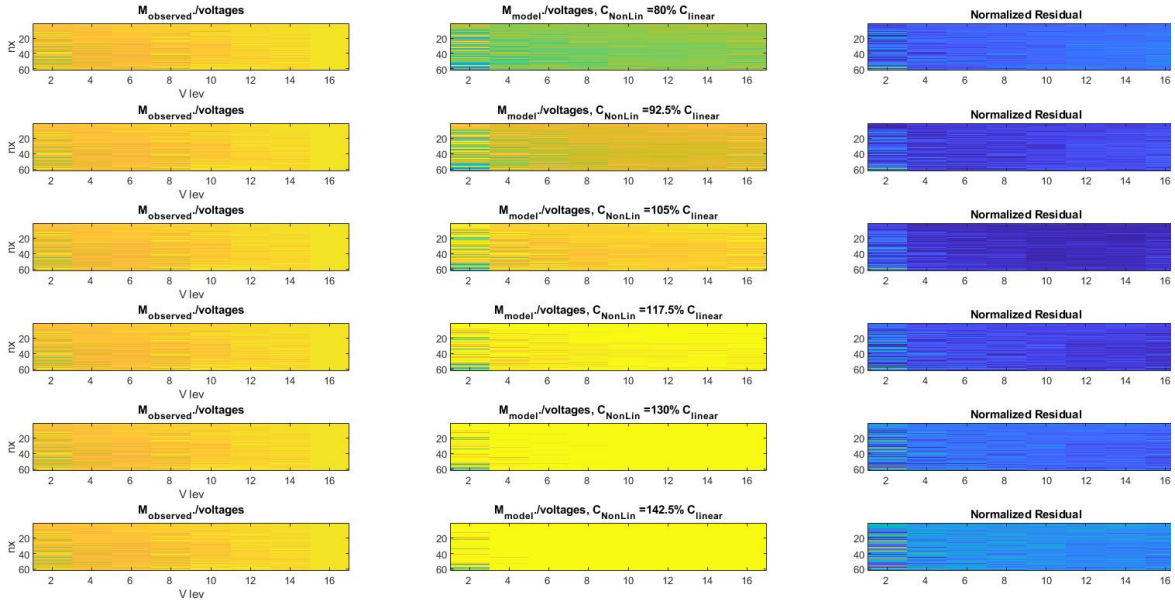

Figure 5-32: Clay Model, Observed and Residual matrices (columns) for different p values (rows).

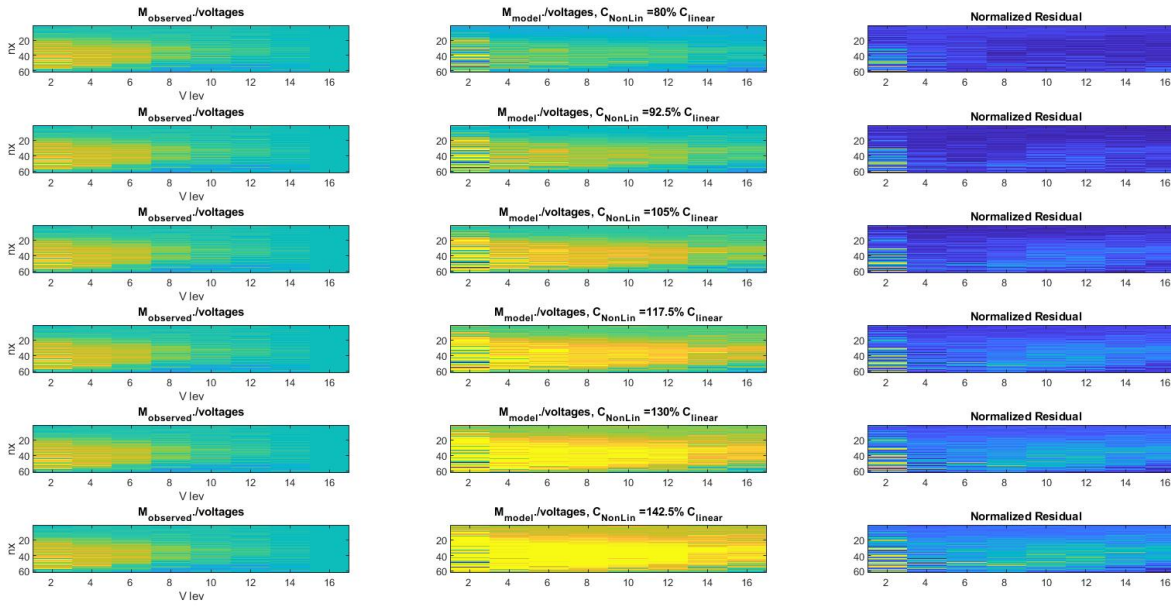

Figure 5-33: Sand-Clay Model, Observed & Residual matrices (cols) for varying p values (rows).

different values of p the minimum residual between $M_{observed}$ and M_{model} could be estimated. The equations used are as follows:

$$Residual = M_{observed} - M_{model} \tag{5-35}$$

With the help of Figures 5-32 and 5-33, we could qualitatively and quantitatively describe the behaviour of the soil signal under the sweeping source stress and identify possible non-linearity behaviours of the soil.

One way of quantifying how non-linear a model is is to compare its non-linear coefficient, C_{NL} with the linear coefficient, C_L. As explained before, $C_L = 2$, so the point is: how many times C_L is C_{NL}? To answer this, we can also consider its percentage of C_L. In fact, we labelled the plots in the preceding figures using percentage of C_L values. The vector of coefficients is our input to the minimization "algorithm", while the output is the index of the coefficient that produces the minimum residual. From this index we could identify the C_{NL} value and consequently, derive the value of the non-linearity parameter, p. Expressed in equations:

$$C_{NL} = 2^{p_{min}} \tag{5-36}$$

$$p_{min} = log_2[2 \cdot perc_{CL}] \tag{5-37}$$

where C_{NL} is a decimal number, not a percentage. Here $perc_{CL}$ is the array of all the percentages of the linear coefficient C_L we want to study. So, for example, we compute p by inverting equation 5-36 for a coefficient $C_{NL} = perc_{CL} \cdot C_L/100$. If it is close to 1, then it is behaving linearly, otherwise it is not. To combine the mathematical derivation of the minimum with the visualization of the residual magnitudes, you can look at Figures 5-32 and 5-33. They must be coherent with the estimated results.

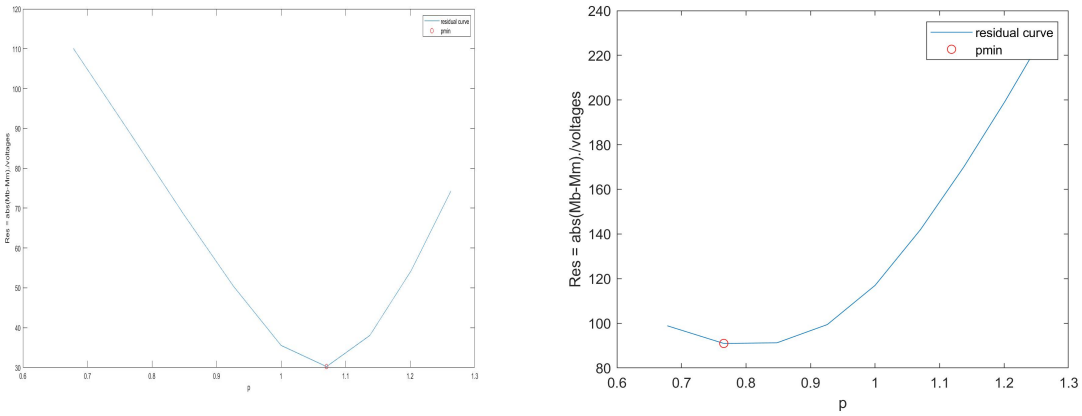

Figure 5-34: Summed residual value curves for (a) Clay and (b) Sand-Clay.

We are still not completely satisfied, because we want to characterise qualitative and quantitatively the non-linearity of the soil. Until, this point, we describe a function dependent to the parameter p that is not really connected with the description of the behaviour. Therefore, we defined a new parameter called γ, the non-linearity parameter. γ has a threshold value that distinguishes the non-linear model from the linear one. The definition is as follows:

For the linear case,

$$2^p = 2^1 \tag{5-38}$$

$$p = 1 - \gamma \tag{5-39}$$

$$\gamma = 1 - p \tag{5-40}$$

If $p = 1 - \gamma$, then $2^p = 2^1 == 2^{(1-\gamma)}$. Therefore, $p = 1 - \gamma$.

We can generalize like this:

$$\gamma = p_L - p_{NL} \tag{5-41}$$

Thus, the non-linearity parameter is defined as the difference in exponential coefficient between the linear and the non-linear model considered.

A spontaneous deduction would be that the sign of γ could be considered a threshold for going from linear regime to non-linear regime. Actually, we should be careful not to jump to any conclusion, because it could be less straightforward. The general formula for γ suggests three cases:

- $\gamma = p_{Lin} - p_{NL} > 0$
- $\gamma = p_{Lin} - p_{NL} < 0$
- $\gamma = p_{Lin} - p_{NL} = 0.$

The trivial case is the point c for which $p_{NL} = p_{Lin}$ and then the behaviour is linear. If $p_{NL} < 0$ then $\gamma > 0$, while if $p_{NL} > 0$, γ can be both positive or negative, depending on the value of p_{NL}. On one hand, we can assume that $p_{NL} > p_{Lin}$ is true and in the case of

positive p_{NL}, γ will be negative. On the other hand, if $p_{NL} > p_{Lin}$ is valid then γ can be only a positive number. As a result, more than focusing on the sign, it is wiser to look at the magnitude of γ. Then we can change its definition by taking just the value of the difference. Thus, the new definition will be:

$$\gamma = |p_{Lin} - p_{NL}|. \tag{5-42}$$

As a consequence, the quantification of the non-linearity behaviour will be based on a positive scale that identifies the grades of non-linearity with increasing gravity from null onwards. So, if γ is small the behaviour is almost linear, if γ is big then the behaviour is not linear (assuming that the linear model is correct, obviously).

The final section of the analysis of the non-linearity with respect to the amplitudes is theoretical. We would like to visualize the model curve with respect to the non-linearity parameter. Therefore, we plotted the general function f(γ) (where γ took the place of x in equation **??**) and the curves of the linear theoretical model and the best fit non-linear model. Figures 5-35 and 5-36 highlight the linear and non-linear with blue and red plus signs along their curve.

In conclusion, we define the general function of the model in this way:

$$f(\gamma) = 2^{(1-\gamma)} \cdot M_{observed}. \tag{5-43}$$

For $\gamma = -1$, $f = f_{linear}$, otherwise $f = f_{nonlinear}$.

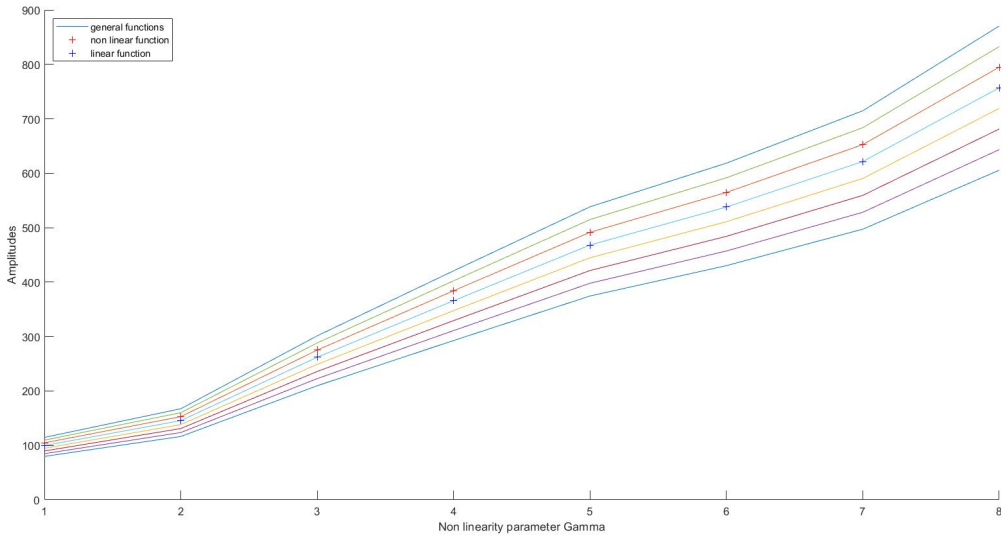

Figure 5-35: Theoretical curves for the Clay model.

Non-linearity with respect to the Voltage level (time-lag analysis)

For the second kind of analysis, just the raw data from the LDV were used as starting inputs. The aim was to recreate the Figure 4.b of Boaga [2021] to see if we could recreate the same experiments in the smaller scale of the laboratory with our two layer analogue model. Therefore, we plot the data recorded at a central point along the line for all the voltage levels.

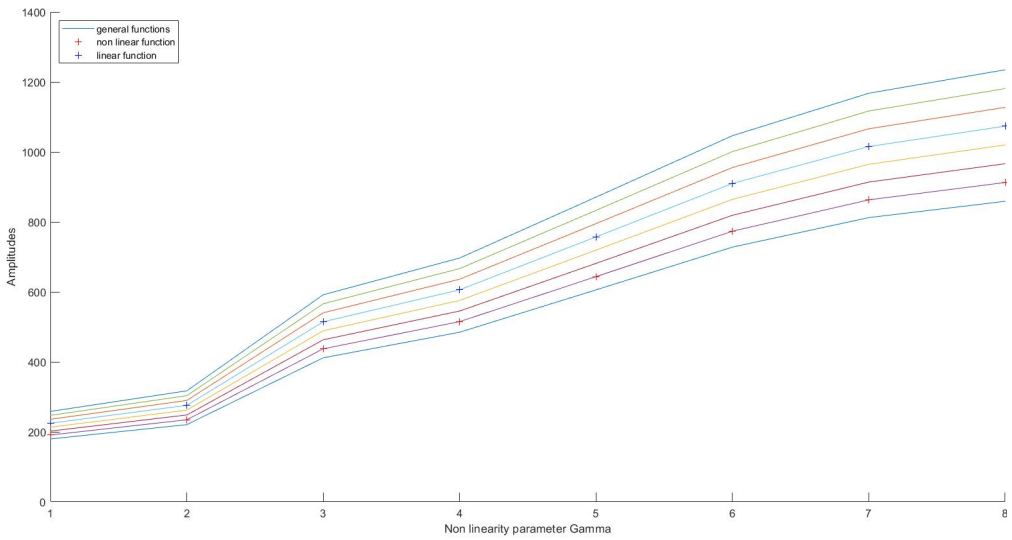

Figure 5-36: Theoretical curves for the Sand-Clay model.

Figures 5-37 and 5-38 show the raw data recorded, while Figures 5-39 and 5-40 are zooms on one period of the soil amplitudes normalised by their voltage level values. Those figures gave us a qualitative result of the non-linearity of the soil. In other words, they display the change of the signal with voltage levels in terms of lag in time and amplitude modulus.

It is possible to derive a general relationship between the response of the soil and the voltage level of the source and to define the type of behaviours of the soil response by comparing the quantitative results of the $Res_{M,norm}$ matrix and the qualitative results of Figure 5-40.

5-2-5 Results and interpretation of Experiment 3 and 4

Non-linearity with respect to the Amplitudes

As for Experiments 1 and 2, the material absorbed a great part of the source input, as evident in Figures 5-23b and 5-23b. This time the source is a sweep and not a burst as in the case of the grid experiments. Thus, each point along the line recorded a different signal for the different voltage levels. Note that the signals were normalized to the voltages values. We can visualized the signal on a fixed point for all the voltage levels in figures 5-27a and 5-27b. On the other side, we can also fix a voltage level, in this case V level=3, and see how the signal change with the distance from the source in figures 5-26a and 5-26b. As expected, the amplitudes decrease with the distance to the source. The closer points to the source have the higher amplitudes, while the last of the line has the smallest. This behaviour must be taken in mind because it is important for the building of the amplitude model of the soil signal. However, the peaks of the signals are shifted from the source signal, but from the figures, which we referred before, is difficult to say how much and with which relation. ΔI and M helped us in that. If the signal was not shifted from the source, then ΔI would have been zero, but this is not the case. For the clay box ΔI is negative, so it means the signal gets

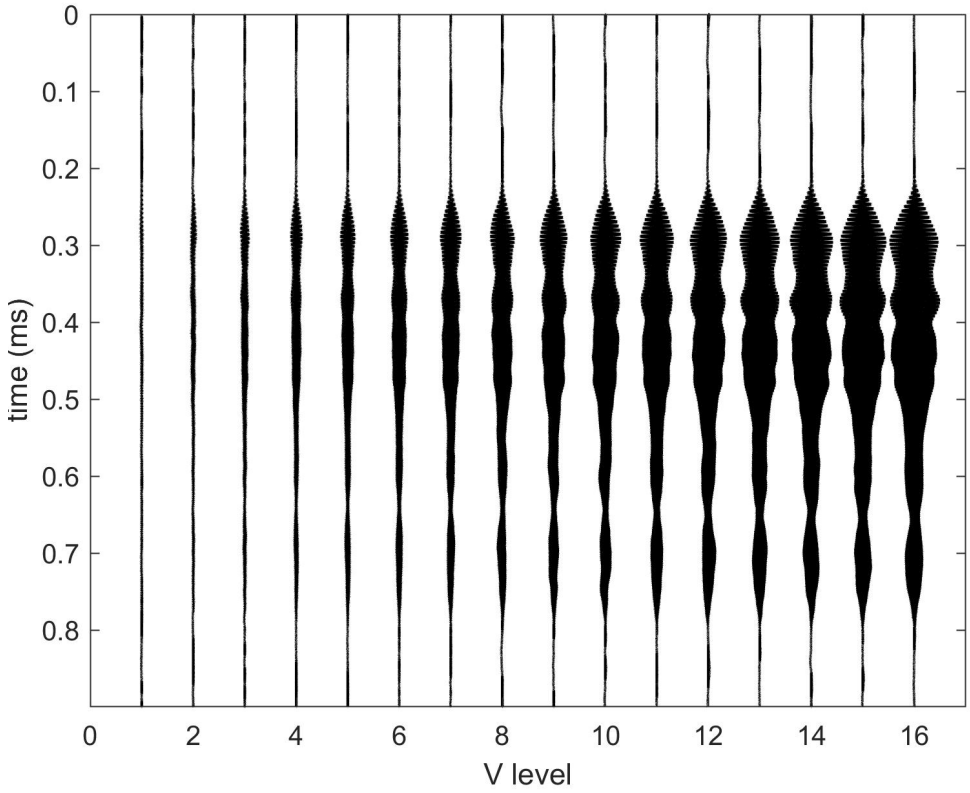

Figure 5-37: Amplitudes for Drive levels Clay

faster with increasing of voltage level, while in the sand case is both positive and negative. Four main vertical groups can be identified in the matrix of the Clay (see figure 5-30). The voltage level between 1 and 5 is around -8, while between 5 to 10 is around -4, from 10 the value goes to zero. From this analysis, we can state that the shift decreases with the voltage level. So, the sand-clay box has a totally opposite behaviour of the clay box. We will have the confirmation of our interpretation by the Non-Linearity analysis respect to the Voltage level with the figures 5-39 and 5-40. It is fundamental to stress that the shift we can identify is not due to the different distance from the source. As we explain in the paragraph **??**, we shifted the signal of the traces at the starting time of the source. So, the shift is an answer of the material to the source input, how it reflected the wave. ΔI of the two layers model shows a peculiarity in figure 5-31. Focusing on the top part of ΔI, its values are only positive. The matrix is mostly green coloured, around two difference in index, except for a relevant yellow shade, related to a bigger value, on the bottom of the figure. The index of the peak increases with the position, but also with the voltage level. The ΔI is maximum for the first 5 voltage levels and becomes smaller and smaller for the greater voltages. Therefore, we can say that the signal gets slower with the voltage level. Again, we will have confirmation of our interpretation by looking to figures 5-39 and 5-40.

Besides, talking about the magnitudes of the maximum of the signal, we can focus on the M matrix in the figures 5-30 and 5-31. The matrix's amplitudes decrease with distance from the source for both experiments, coherently with figures 5-26a and 5-26b and with our

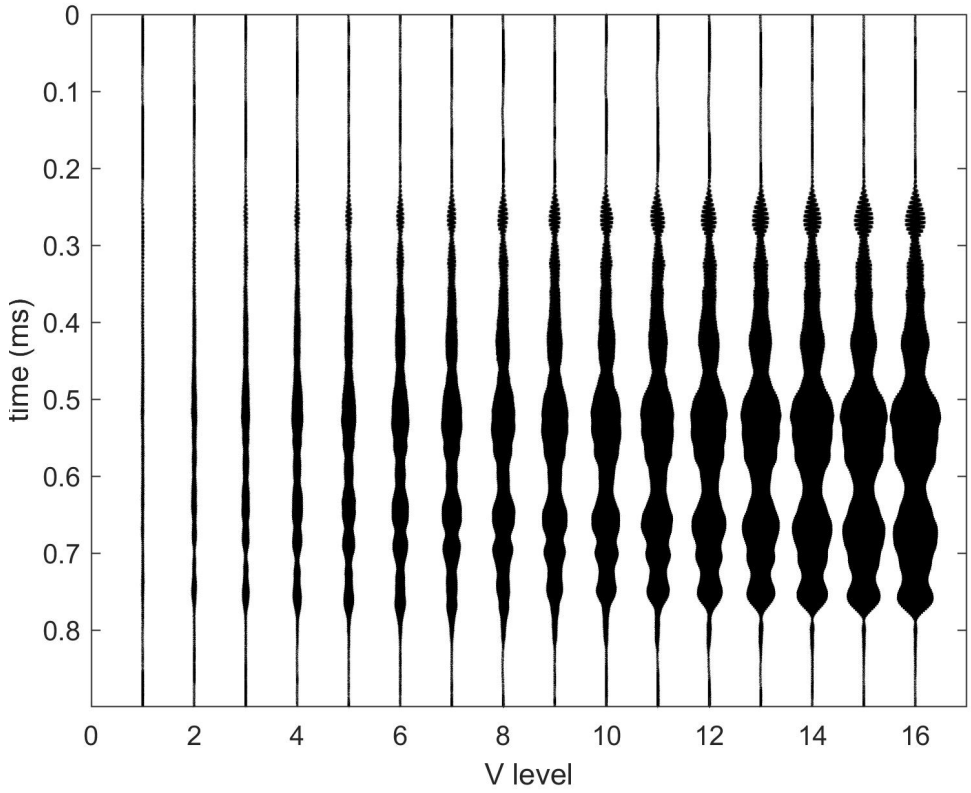

Figure 5-38: Amplitudes for Drive levels Sand

expectations. The matrix M of the clay box has the variation clearer. The reason is that the first point of the line has an amplitude out of scale respect to other points. The trace is ruined by the noise. But if you look carefully on the blue colour variations in the sand M, you can see the same decrease of magnitude. The noised trace is evident in figures 5-40,which is the biggest wavelet. After the two normalization we can compare M and it model for the different γ. The six models displayed in figures 5-32 and 5-33 are respect to a C_{NL} that is 80%,92.5%, 105%, 117.5%, 130%, 142.5% of C_L. For the single layer model the non linear coefficient is 105% of CL, while for the two layers model is 90%.

$$C_{NLclay} = 2.1 \tag{5-44}$$

$$C_{NLsand} = 1.7 \tag{5-45}$$

The clay coefficient is approximately $C_L = 2$, then we can say that the one layer model behave linearly. From the minimum residual and the non linear coefficient, we can derive the p_{min}, which are:

$$p_{minclay} = 1.07 \tag{5-46}$$

$$p_{minsand} = 0.77 \tag{5-47}$$

And then their respective non linearity parameters:

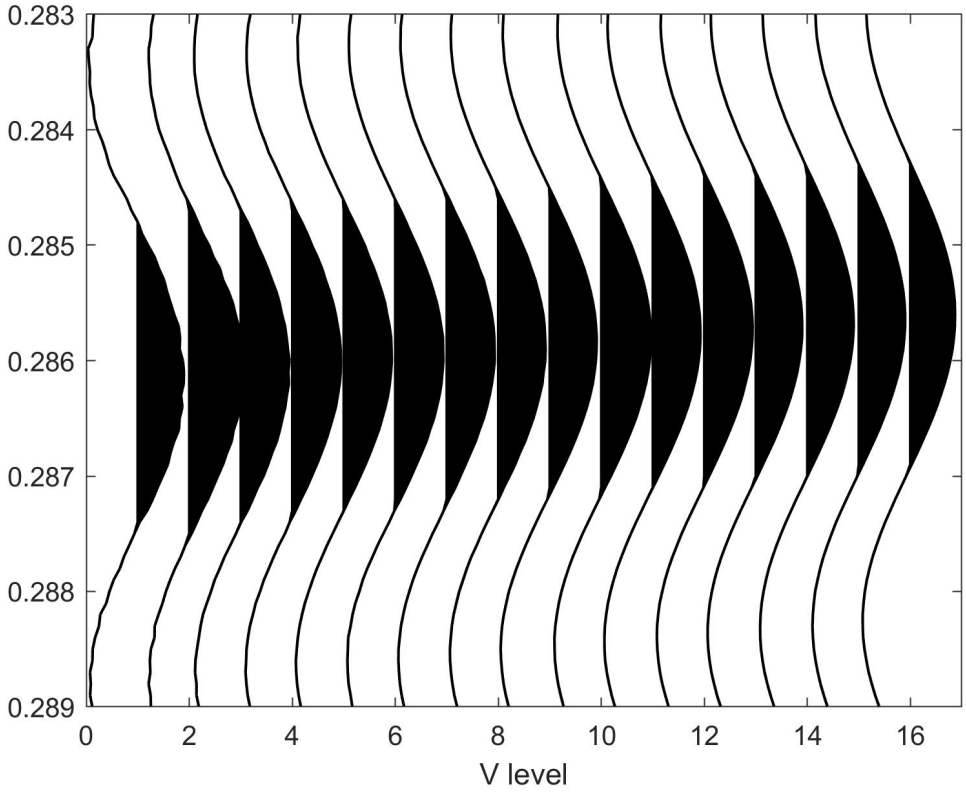

Figure 5-39: Zoom and scaled Normilized Amplitudes for Drive levels of the Clay

$$\gamma_{clay} = 0,07 \tag{5-48}$$

$$\gamma_{sand} = 0.23 \tag{5-49}$$

The comparison between the experiment 3 and 4 helps to better understand the threshold between a non linear and a linear behaviour of the soil. The clay box has a C_{NL} approximately of 2, and its non linearity parameter has an order of magnitude of 10^-2; while for the sand box's C_{NL} is smaller than the clay's box and its non linearity parameter is one order of magnitude bigger than the module of γ_{clay}. Thus, the interpretation of that could be that the two layers model behaves more non linearly than the single layer model
It would be interesting to see the soil response like a function of γ . Understanding how the material changes the response enable to define the physical law for the nonlinear regime. Generally, we have a material that is stressed by a ground motion. dependently to the magnitude of stress. However, we just saw that the clay box has a linear regime with the same source input as the sand-clay model, but the last one has a non linear regime. Thus, there is something more than the relationship with the source input. Why only the clay? Why the sand reacts differently? What is the difference between clay and sand? A simplification of such complex system like the two layers model might be a box of two subsurface. One homogeneous, the other heterogeneous with small grains of different sizes. In our case the deeper subsurface is the clay, while the shallowest is the sand, which has grain from 0. And 2

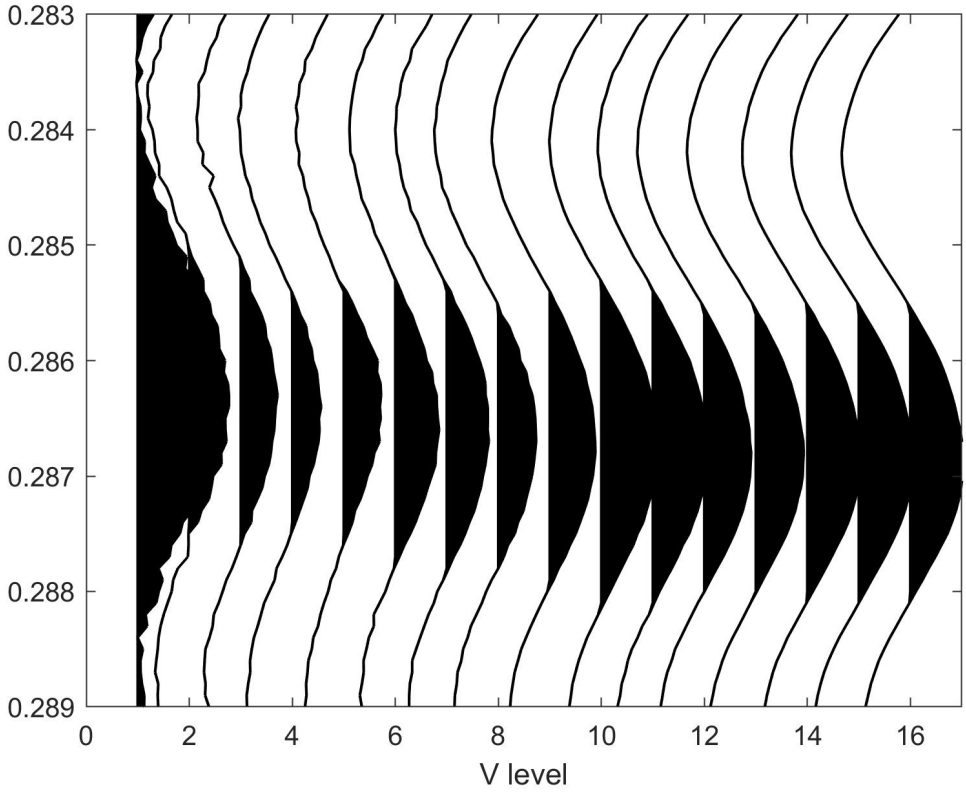

Figure 5-40: Zoom and scaled Normilized Amplitudes for Drive levels of the Sand

mm of diameter. Whereas the single layer model is just a homogeneous layer of clay. Now, if we imagine a source shakes the two models in the same way, and if we just consider the waves like a ray scattering in the mediums, then we can clearly deduct the rays would take different paths in the two experimental boxes. The ray would have had much more work to do to go through the first and second layer, rather than in the clay box. The grains behave like second sources that spread and reflect the rays everywhere. Therefore, their presence in the medium must influence the phenomena somehow. The example of the homogeneous medium makes us imagine better that the ray would have scattered just at the end of the model, because no obstacles were inside. Obviously, the phenomena is much more complex, but it might help to understand that the grains and the heterogeneity of the shallow layer have luckily a influence on γ, therefore on the non linear model shape. Another point to keep in mind is that we choose a second layer with a greater density and compaction level rather than the first layer. For instance, the previous field works worked with sandstones or limestones over sand or quartz (remember chapter 3), materials lighter and less compact. We recreated an analogue model in small scale of the laboratory. The second layer behaves like a base for the first, its characteristic response to the signal remain unaltered from experiment 1 and 2, as you can see comparing Figures 5-6 and 5-17. The clay reflects waves upwards from the sand-clay interface as we saw in figure 5-10 and in 5-14. Those reflections influence the direct waves and the reflected wave, too, but only locally, they do not deform the signal in a way that the amplitudes slow down. Consequently, we can deduct that the bottom harder layer

does not induce the non linearity directly, a part for the only rule of not make sinking the shallow layer under the source shake. On the contrary, if the bottom layer were less compact and dense than the first layer, both would have collapse under the source position and the source would have been buried. To avoid that, we choose this set up. Besides, going back to the main topic, the nature of γ, a possible dependency on the density difference of the layer is out of consideration. Therefore, γ might be a function of the sand properties, only. We suggest the non linearity parameter is dependent to the first layer material properties, so its geometrical and hydroelectric parameters, for example the level of heterogeneity, the size of the grains, their distributions, as well as the water content, the porosity. As a result, the scale for gamma may go from $\gamma = 0$ for the theoretical homogeneous material to $\gamma = 0.15$ for the heterogeneous material with grains of on the millimetre scale, of a certain low moisture level, with a considerable porosity. The precise estimation of those parameters is out of the thesis's topics and we recommend future projects to focus on that. Anyway, to generalize the concepts we exposed until now, we could write γ as a function in the following way:

$$Model(2 * V) = (2^{(1-\gamma)}) * M_{observed}(V) \tag{5-50}$$

$$\gamma = f(size\ of\ grain,\ distribution\ of\ grain,\ heterogeneity,\ moisture\ content,\ porosity) \tag{5-51}$$

In conclusion, the non linearity behaviour of the soil is dependent on the geometry of the model, in particular is strictly dependent on the presence of micro grains and their distribution inside the shallow sublayer of the model. We suppose there may be a connection with the hydroelectric characteristics of the medium, too, but it is out of the scopes of the thesis proven it. By plotting the model respect to the γ values we can see how the curve changes, looking at Figures 5-35 and 5-36. The crossed blue and red curves are respectively the linear model and the non linear model of our experiment 3 and 4. What is important to underline is that the model suggested is a one order linearization. The coefficient may include also other terms of bigger order that we ignore. A more accurate linearization of the model should include other parameters and variable, like for instance the relationship with the friction between the micro-grains ([Johnson and Jia, 2005]), the water content ([J. A. Ten Cate, 1996]), the second order non linearity coefficients like the paper of Brunet and Johnson [2008] did for the strain estimation in a non linear contest. If we included the order of linearization the complexity of the problem would increase as well as the unknown variable, then we decided that the first order was the best linearization possible for our project, mainly due to time limits.

Non-linearity with respect to the Voltage level (time-lag analysis)

The combination of the results of the amplitude analysis (5-2-5) and the voltage level analysis explains the non linear behaviour of the soft soil. If the results match, then we have a proof that how interpretations might be at least coherent and may be correct.

Figures 5-39 ,5-40 display the normalized velocity amplitudes respects to the voltage level at a fixed point along the line for a finite time window. Each wavelet is for a different voltage level, so you can analyse the evolution of the signal with the increase of the voltage level. It is evident that for the trend is upwards for the amplitudes of the clay box. Thus, the wavelet go faster with the increase f voltage level. On the other side, the sand-clay box experienced a total opposite event: they go downwards, or in other words, the wavelets go slower with the

increasing of voltage level. Figure 5-39 shows the linear behaviour of a material under stress, while Figure 5-40 represents the non linear behaviour. What is fun to note is that the first definition of γ has the sign involved, and the clay model has a negative values (-0.07), while for the two layers model it was positive (+0.15). It may be a case that for the slope of the clay is negative, while the sand-clay model's is positive slope? We keep the question open because to be able to verify that, we should had made experiments with different materials or at least comparing more than two models. However, what is relevant is the affinity with the voltage and the amplitude analysis. In fact, ΔI mirrors the signal behaviour respect to the voltage level. By comparing Figures 5-30 and 5-39, we can identifying the shift in index in ΔI in the lag of the signal in the wavelets figure. ΔI increase the lag with the decreasing of voltage level, as well as the signal gets slower with decreasing of voltage level in Figure 5-39. Doing the same for the two layers model, we can see that in Figure 5-40 the signal gets faster with the decreasing of voltage level as well as the lag is bigger for lowest voltage levels than for the highest. The matrix M contributes to the interpretation, too. About the sand, Figure 5-31, the first row of M is yellow, much higher amplitudes than the rest and that matches Figure 5-40 the first wavelet at the lowest voltage level is almost out of scale, deformed by noise. Figure 5-33 show it too for voltage levels 2, for the case of non linear coefficient 92.5% of the linear one.

However, the crucial point is that the signal is dependent to the voltage level non linearly for the two layer model. We demonstrated that the non linearity behave was recreated with our analogue model in laboratory and seen on our data.

Chapter 6

Conclusions

To summary, the experiments carried out enable to understand, to qualitatively describe, and to quantify the non-linearity behaviour of the analogue soft-soil model constructed in the laboratory. The main goal of recreating and seeing the non-linearity for a soft-soil layer overlying a harder bedrock layer in an intermediate-scale laboratory experiment was thus reached.

Reaching this goal required establishing the behaviour of the particular analogue materials chosen (i.e., Clay and Sand) to reproduce the field setup and, in particular, to carefully consider their scaling behaviour. While a full dynamic scaling analysis would require carrying out a matching field experiment, and was therefore beyond the scope of the thesis, the materials used were characterized in detail through impulsive experiments, both separately and jointly.

For the non-linearity experiments involving frequency swept sources, new, cross-correlation based processing approaches for separating propagation-related phase changes from source-level induced propagation delays were developed. We also defined a new parameter called the non-linearity parameter, γ, that allows characterizing the soil for its type of non-linear response on a positive scale, where zero corresponds to the theoretical behaviour. We tested that until $\gamma = 0.07$ the linearity is held, while for values close to one, such as in the case of experiment 4, with $\gamma = 0.85$, the regime changes to non-linear. We suspect a threshold exists, which defines the switch from the linear to non-linear regime, but we could not define a precise value. More experiments with different models and materials should be done to determine the threshold value of γ.

The results obtained make us somewhat confident to state that the non-linear regime is most probably induced by the presence of micro grains in a soft, thin, heterogeneous medium overlying a thicker, harder medium that allows the scattering of the source input without permanently deforming the shallow layer and without burying the source. We believe that the size of the grains, the distribution of the grains in the medium, and the geometry of the experiment all play a fundamental role in the response, to the point that it can slow down the signal with increasing voltage level.

The crucial point is that we demonstrated that the signal is dependent on the voltage level in a non-linear way, both from the analysis of the response's amplitudes and the analysis of their

lag with respect to the input voltage level. Moreover, the residual (Res) highlights the peculiar response of the analogue model, computed by the difference between the theoretical linear model of the maximum amplitudes (M_{model}) and the observed data ($M_{observed}$). With help of the estimation of the minimal residual, we derive the non-linear coefficient and consequently the non-linearity parameter, γ, that allows to build the best fit for the model of the experiment. Thus, we not only verify the existence of the non-linearity behaviour of the soft soil, but we could also describe it with a general physical function dependent on the voltage level and on γ. It appears that the non-linearity parameter is strictly connected with the geometry of the soft material. γ is a function of the size and the distribution of the grains inside the soft layer. The general function describing the non-linear behaviour of the Sand-Clay box can thus be stated as follows:

$$A(2 \cdot V) = 2^{(1-\gamma)} \cdot A(V), \tag{6-1}$$

where

$$\gamma = f(\text{size of grains, distribution of grains, compaction of the material, etc.}). \tag{6-2}$$

The general functions with respect to gamma are displayed in Figure 5-36. The tendency towards exponential curves is evident, but the slope is dependent of the value of γ, and therefore on the type of material. Furthermore, the Clay box, i.e., experiment 3, appears to behave linearly and our thesis is that homogeneity of the medium prevents reaching the non-linear regime, even if the source signal is the same as in experiment 4. Of course, if the stress and strain level should reach a certain value, for example, if the shear strain should exceed $10^{-}6$, then it could also behave non-linearly. But even if we used the same source on the clay, the non-linearity was not seen.

In conclusion, the non-linearity behaviour affects both the magnitude of the amplitudes and the arrival time of the signals, providing an intensification of the amplitudes and a lag in time of the wavelets. An exponential factor links the signal to the voltage level and it is possible to linearize the response function by multiplying with a logarithmic factor in base 2.

Not only was the main aim of the thesis reached successfully; the qualitative description of the non-linearity of the soft soil and the correct recreation in the intermediate scale of field works in the laboratory through an analogue model, but we managed to generalize the phenomena giving for the first time a physical description introducing a new parameter that identifies the level of non-linearity of the material. We are pleased with this result, because many papers on the topic appear to lack a physical description of the phenomena. The hope is that this research project could be a valuable starting point for a further experiments in the intermediate scale for and novel classification techniques for non- linear materials.

Chapter 7

Outlook

The results obtained in the thesis highlight many possibilities to improve the model chosen. Mainly due to lack of time and also materials, we had to delimit the research to the four main experiments, using only two types of models. Of course, this ultimately limits the results.

The recommendations for future works are many. Firstly, repeating experiments 1 and 3 for different models, for example, with different materials of greater or smaller mass density and compaction, or maybe with more layers, such as, for example, three or four layer models. It would allow verification if the difference in density and the compaction influence γ as well, or if the non-linearity happens just for the top (sub)layer. Then the materials chosen could be different in size and distribution of grains, so that γ can be treated as a function of the diameter and the density of grain per millimetre. A correlation analysis could be done in order to improve the model and maybe introduce new parameters in the general function. The analysis could be repeated for water content and porosity. The same analogue model studied dry could be filled with water to increasing percentages, until the saturation level, and see if the non-linearity regime changes its characteristics.

Furthermore, we ignored the internal friction of the grains, the internal thermal energy, the change of distribution of the grain in the medium, viscosity, hysteresis, Hertz's non-linear contact theory, conditioning and many others, see e.g., Johnson and Jia [2005], P. A. Johnson [2005], J. A. Ten Cate [1996], Brunet and Johnson [2008], as already introduced in chapter 2.

Therefore, a truly general function for the non-linear regime can be described as follows:

$$M_{model} = \Big[2^{(1-\gamma)} + f(d) + g(n) + h(\phi) + k(w) + l(strain) + m(friction) + o(T) + \ldots\Big] \cdot M_{obs}(V),$$

where d is the diameter of the grain, n is the density of grains in the volume, ϕ is the porosity, w is the water content, T is the temperature (and f, g, h, k, l, m, and o are general functions). This equation shows the complexity of the non-linearity problem. If the threshold between linear and the non-linear regime is found, it might be possible to classify the materials based on their non-linearity levels and to introduce a new geophysical classification of materials never seen before.

Another point would be focusing on the estimation of the strain of the source or even the strain as "felt" by the soil. Understanding the correlation between strain, voltage level of the source and amplitude response of the model can certainly give more information to optimize the setup of the experiment. As well as it would help to derive other geotechnical parameters in-situ, such as, for instance, the Young's moduli of the soil. However, how to estimate the strain in-situ is an open question. As mentioned previously, new developments in fiber-optic sensing could have a role to play here. And then, if a future team would work on two scale experiments simultaneously, one in the field, and one on the intermediate scale in the laboratory, an outlook would be finding a way to estimate the strain, in particular the shear strain, appropriate for both the large and intermediate scale experiment. We already suggested to look at the recent works of Dr. Edme and Prof. Robertsson from ETH for that. Starting from those results, it would be very interesting to check the dynamic scaling and compute the Elastic Proportional Coefficient. Is it influenced by the non-linearity behaviour or more by the setup chosen? Was the analogue model scaled correctly? Etc.

As we have already mentioned in Chapter 3, our project tried to answer two main questions: Is it possible to recreate an active seismic survey in an intermediate scale experiment in the controlled environment of the laboratory? And: How to qualitatively and quantitatively describe the non-linearity behaviour of the soil? We answered them, but at the same time the results opened many new questions. We just listed here the few ideas we considered more relevant, but the "outlooks" could be many more than that.

Bibliography

J. Boaga. Multi-drive level vibroseis test to evaluate the non-linear response of soft soils. *Soil Dynamics and Earthquake Engineering*, 81(149):1–11, 2021.

X. J. Brunet, T. and P. A. Johnson. Transitional nonlinear elastic behaviour in dense granular media. *Geophysical Research Letters*, 35:L19308, 2008. doi: 10.1029/2008GL035264.

S. Cecchi. Proposal of master thesis project with eth by stella cecchi. 2022.

M. K. Hubbert. Theory of scale models as applied to the study of geologic structures. *Bulletin of the Geological Society of America*, 48:1459–1520, 1937.

T. J. S. J. A. Ten Cate. Slow dynamics in the nonlinear elastic response of berea sandstone. *Geophysical Research Letters*, 23(21):3019;3022, 1996.

P. Johnson. URL https://public.lanl.gov/geophysics/geophysics/staff/johnson/johnson.shtml.

P. Johnson and X. Jia. Nonlinear dynamics, granular media and dynamic earthquake triggering. *nature*, 437, 2005. doi: 10.1038/nature04015.

P. A. Johnson. Inducing in situ, nonlinear soil response applying an active source. *JOURNAL OF GEOPHYSICAL RESEARCH*, 114:1–14, 2009.

C. A. L. F. P. J. G. P. A. J. F. Y. M. Lawrence, P. Bodin and T. Brackman. Induced dynamic non-linear ground response at garner valley, california. *Bull. Seismol. Soc.Am.*, 98:1412 – 1428, 2008.

Z. Lawrence. URL https://www.linkedin.com/in/zachary-lawrence-8974978a/.

A. S. P. A. Johnson. Slow dynamics and anomalous nonlinear fast dynamics in diverse solids. *The Journal of the Acoustical Society of America*, 11:124–130, 2005. doi: 10.1121/1.1823351.

S. D. H. I. D. S. T. T. F. B. M. H. C. V. R. J. W. Schmelzbach, Cedric and J. Robertsson. Advances in 6c seismology: Applications of combined translational and rotational motion measurements in global and exploration seismology. *Geophysics*, 83(3):WC53–WC69, 2018.

H. I. C. S. P. E. D.-J. V. M. F. B. S. Y. J. W. U. S. Sollberger, David and J. O. Robertsson. Seismological processing of six degree-of-freedom ground-motion data. *Sensors*, 20(23): 6904, 2020.

V. G. V. N. P. B. V. Tournat, V. Zaitsev and B. Castagnède. Probing weak forces in granular media through nonlinear dynamic dilatancy:clapping contacts and polarization anisotropy. *Physical Review Letters*, 92(8):085502, 2004. doi: 10.1103.

P. Z. Lawrence and C. Langston. In situ measurements of nonlinear and nonequilibrium dynamics in shallow, unconsolidated sediments. *Bulletin of the Seismological Society of America*, 99(3):1650–1670, 2009. doi: 10.1785/0120080177.

Appendix A

Additional comments on the computation of ΔI

In chapter 5 at section 5-2-4 we described the processing method created to analyse the data. The non linearity of the signal was studied through the time shift of the received signal and the amplitude deformation, respectively represented by matrices ΔI and M. In this appendix we would like to clarify and justify the estimation of the matrices only for a specific time window.

The matrix equation 5-26 defines ΔI as the difference in time of the source and the output signal in a specific time window, that we can called "tw". M is the max amplitude in the time window tw, as well. Thus, our matrices do not represent the total lag of the soil signal and the maximum amplitudes for the whole signal, but just in a small time window. Somebody could ask why we did not do it for the whole acquisition time, and maybe if the results of the residuals with those matrices can really represent the behaviour of the soil.

Firstly, we remind the method used. We look at the whole soil signal for all the voltage level in one point (look at Figures 5-27a and 5-27b) and then we zoomed in the middle part and we focus on one wavelet period. We decided to take the part in the middle due to the nature of the sweeping source. That starts from a very low amplitude and reaches a very high amplitude in a short period. Therefore, the signal varies a lot at the begging and at the end of the sweep, while the main body is constant at the amplitude we wished (see Figures 5-24a and 5-24b). The reason why we computed the matrices only for a period of the wavelet is because we wanted just one value for each receiver and each voltage level. So, practicality is the answer for the first question. For instance, you could also build a big M matrix and store all the maximum of the signal, but than it will be time consuming and it will not give you a better analysis. It would be much more difficult to handle such matrix and it will not give so many relative extra information on the non linearity behaviour of the soil. Therefore, we consider enough good to look only at a part of the signal as representative for the whole.

However, we did a "check test" to verify that ΔI and M could be representative of the behaviour of the soil. It consisted in the estimation and comparison of ΔI and M of the two

layers model for four time windows of the signal; at the head, at the body part, at the tail. For that, we created three tapers that we applied at the sand signal by multiplication. We called them tp1,tp2 and tp3. They are displayed in Figure A-1. The tapered source and sand signals resulting are displayed in Figure A-2 and Figure A-3. There, you can see the signals are divided in three part: head, body and tail.

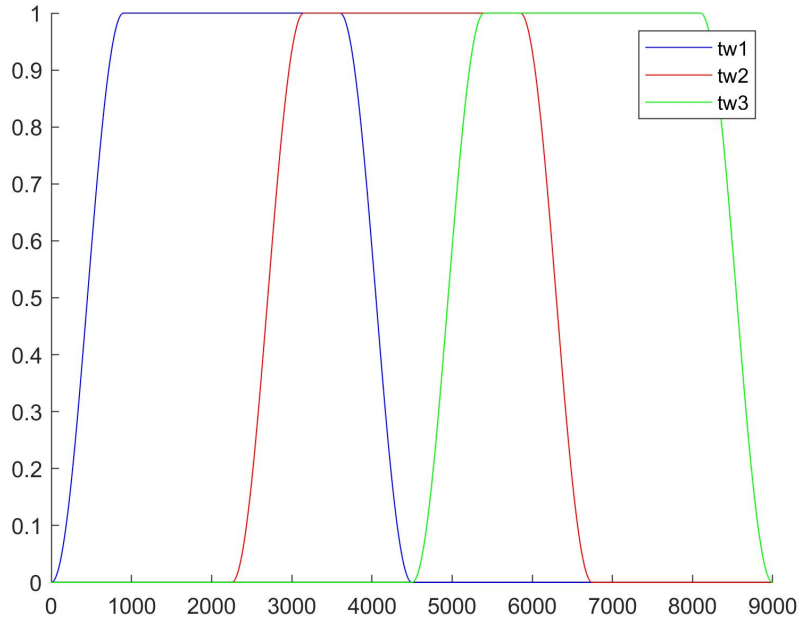

Figure A-1: The tapers we applied on the sand signal

Then, we repeated the methodology for computing ΔI and M, so we focused on a wavelet for a length of its period. We chose four time windows, specifically:

$$tw_0 = [3050, 3090]; tw_1 = [3050, 3100]; tw_2 = [4950, 5000]; tw_3 = [6585, 6615];$$

Note, their are just the index of the times selected not, they are not in seconds. Figure A-4 showed the wavelets we are talking about.

The corresponding ΔI are visible together in Figure A-5, while the M in Figure A-6. About ΔI, overall they all behaviour in the same way. Their modules increase with the distance to the source. For tw_0 the lag is $\Delta I = -1$ at first points of the line, then 3 in the middle and 9 at the last points; for tw_1 there is $\Delta I = 1, 2, 4$, while for tw_3 is $\Delta I = -1, -3, -5$. ΔI_3 is peculiar, because its values change periodically with a pattern similar to a sinusoidal curve. There is a correlation between ΔI and the distance from the source and the voltage level, but we do not know of which nature. Anyway, the point here is that ΔI_2 also increases in modulus with the distance. As a result, the use of one time window to study the behaviour of the soil lag respect to the source signal can be consider as enough. Besides, for a didactic purpose, tw_0 was taken from the same taper interval of tw_1 (tp1) as a example for a wrong selection of the time window. There is a drastic increase of ΔI_0 for the last points, from the

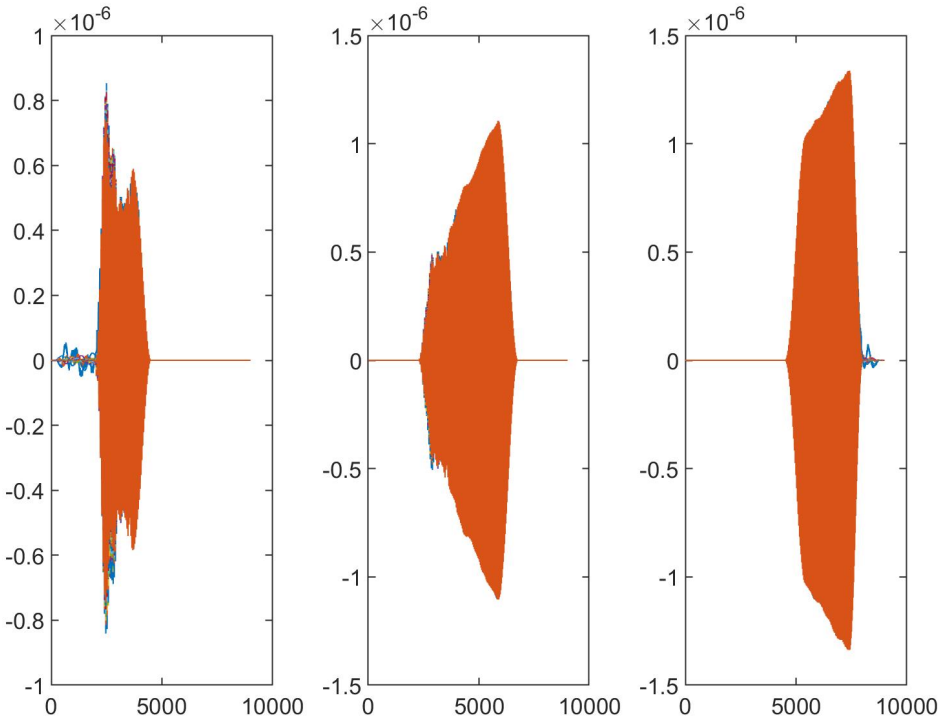

Figure A-2: Source signal in 3 time windows, at the head, at the middle and at the tail of the whole signal

55th and the 62nd. This is not a behaviour of the analogue model, but it is an issue due to the time window chosen. In fact, it means that the last 5 points' peaks are out of the interval. Thus, the best chose for the tapered sand signal with tp1 is tw_1, while tw_0 does not give information for all the points along the line.

More evident and straightforward is the M matrices. They are very similar to each others. Again tw_2 and tw_3 have some internal variations due to the unstable source signal at the end of the sweep. But, all the matrices keep the main characteristics of M.

In conclusion, we demonstrated that the analysis of the non linearity of the soil with ΔI and M estimated on one wavelet period time window is enough to describe correctly the whole body.

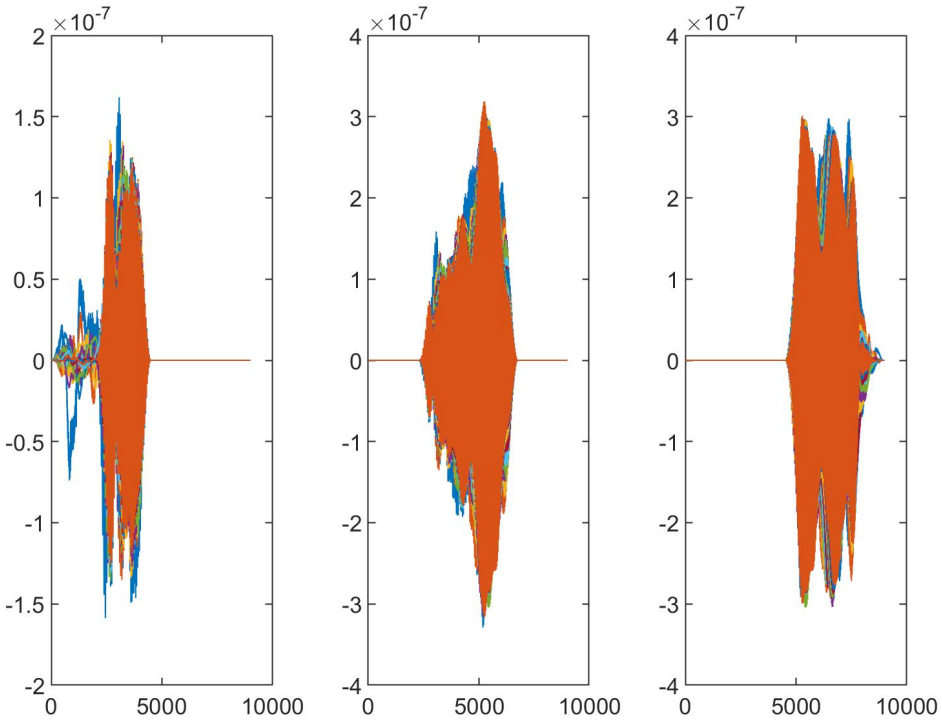

Figure A-3: Sand signal in 3 time windows, at the head, at the middle and at the tail of the whole signal

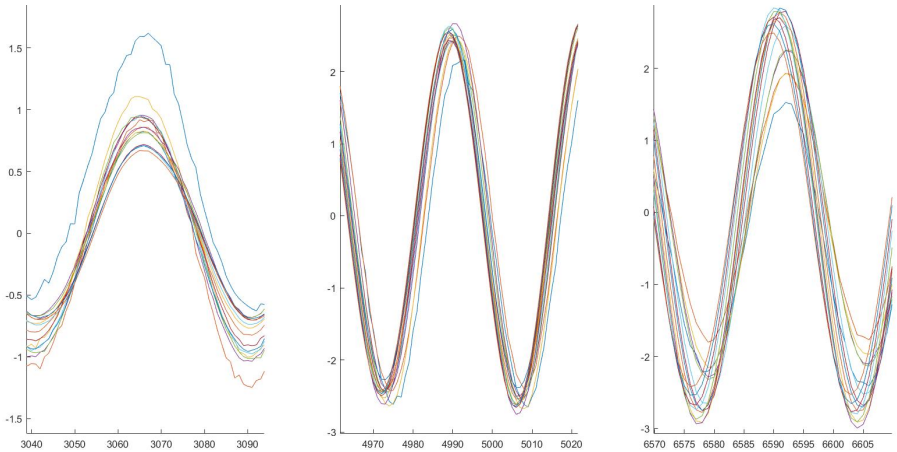

Figure A-4: Zoom on one

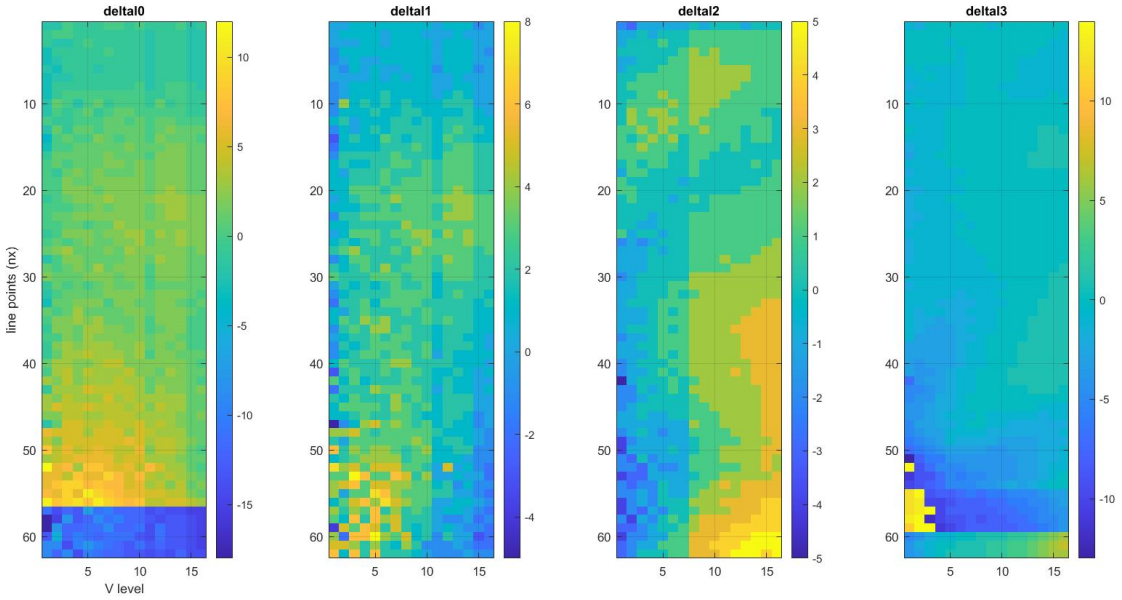

Figure A-5: Comparison of ΔI for four time windows, $tw_0 = [3050, 3090]; tw_1 = [3050, 3100]; tw_2 = [4950, 5000]; tw_3 = [6585, 6615]$.

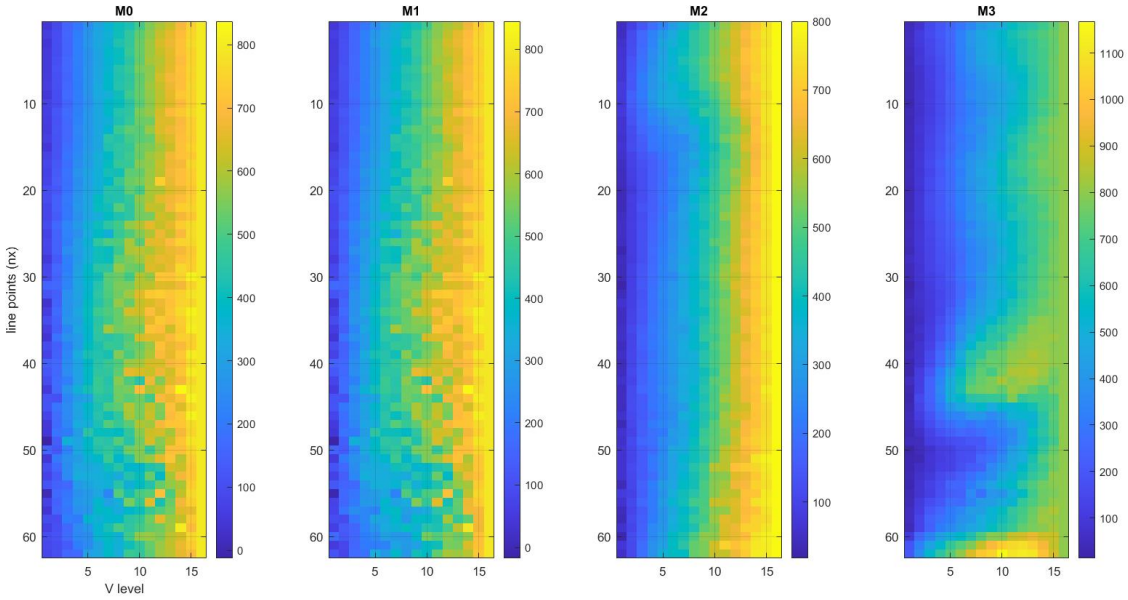

Figure A-6: Comparison of M for four time windows, $tw_0 = [3050, 3090]; tw_1 = [3050, 3100]; tw_2 = [4950, 5000]; tw_3 = [6585, 6615]$.